



Cite this: DOI: 10.1039/d6fo00489j

# Intestinal oxidative stress mitigation and transepithelial anti-inflammatory bioactivity mediated by EtOH-modified supercritical-CO<sub>2</sub> coffee pulp extract

Shuai Hu,<sup>a,b</sup> Miguel Rebollo-Hernanz,<sup>a,b</sup> María Martín-Trueba,<sup>a,b</sup> Vanesa Benítez,<sup>a,b</sup> Yolanda Aguilera,<sup>a,b</sup> María Ángeles Martín-Cabrejas<sup>a,b</sup> and Alicia Gil-Ramírez<sup>a,b</sup>

This research examined the antioxidant and anti-inflammatory effects of ethanol-modified supercritical CO<sub>2</sub> (EtOH-modified sc-CO<sub>2</sub>) coffee pulp extract after INFOGEST 2.0 *in vitro* simulated gastrointestinal digestion. EtOH-modified sc-CO<sub>2</sub> extract digesta (3.1 mg mL<sup>-1</sup>) contained elevated concentrations of protocatechuic acid (61.2 µg mL<sup>-1</sup>) and caffeine (287.6 µg mL<sup>-1</sup>) compared to water and ethanol digesta, contributing to its strong ABTS radical scavenging capacity (4015 µg TE mL<sup>-1</sup>) and superior cellular antioxidant activity (37.8%), along with cyclooxygenase 2 inhibition activity (37.2%). In a Caco-2/THP-1 co-culture model of intestinal inflammation induced by 4 h of LPS (1 µg mL<sup>-1</sup>) stimulation, a 24 h treatment with the EtOH-modified sc-CO<sub>2</sub> digesta (diluted 1:14, v/v, in complete culture medium) demonstrated transepithelial anti-inflammatory effects, decreasing TNF-α, IL-6, CCL2, and IL-1α levels by 9.9%, 24.7%, 34.3%, and 17.0%, respectively, in comparison to the LPS-stimulated control group. Relative to the pure standard mixture digesta, the EtOH-modified sc-CO<sub>2</sub> digesta favored a balance between pro-inflammatory (IL-1α and IL-1β) and anti-inflammatory mediators (IL-10 and IL-1ra), highlighting the importance of matrix effects in inflammation regulation. Bioinformatic analysis revealed that protocatechuic acid, chlorogenic acid, and caffeine metabolites potentially inhibit NF-κB-driven signaling. These results demonstrate that coffee pulp extracts obtained through EtOH-modified sc-CO<sub>2</sub> extraction exhibit substantial bioavailability and bioactivity, reinforcing their potential application as functional food ingredients for the prevention of chronic diseases.

Received 30th January 2026,  
Accepted 22nd March 2026

DOI: 10.1039/d6fo00489j  
rsc.li/food-function

## 1. Introduction

Coffee pulp, which accounts for nearly 50% of the coffee fruit's dry weight, is a primary by-product of the coffee industry.<sup>1</sup> Although often discarded, resulting in significant environmental challenges, recent research highlights its potential as a valuable raw material rich in bioactive compounds. The coffee pulp contains dietary fiber, amino acids, (poly)phenols, and caffeine, which exhibit antioxidant, anti-inflammatory, and antimicrobial properties, positioning it as a promising ingredient for functional food products, nutraceuticals, and other value-added applications.<sup>2,3</sup> In this context, the valorization of coffee pulp through green extraction techniques aligns with

the growing global demand for sustainable and health-promoting food ingredients. Ethanol-modified supercritical CO<sub>2</sub> (EtOH-modified sc-CO<sub>2</sub>) extraction represents a more sustainable and environmentally friendly alternative to conventional organic solvents, enabling the efficient recovery of bioactive compounds while reducing the environmental impact.<sup>4,5</sup> Our previous studies demonstrated that EtOH-modified sc-CO<sub>2</sub> extraction, under optimized conditions (65 °C, 23 MPa, and 9% w/w ethanol), yielded high enrichment of protocatechuic acid (14.9 mg g<sup>-1</sup> extract), chlorogenic acid (0.6 mg g<sup>-1</sup> extract) and caffeine (106.3 mg g<sup>-1</sup> extract) compared to conventional extractions, all of which are associated with significant health benefits.<sup>6</sup> Furthermore, the EtOH-modified sc-CO<sub>2</sub> extract demonstrated enhanced chemical and cellular antioxidant activity in Caco-2 cells and HepG-2 cells, as well as anti-inflammatory effects in RAW 264.7 cells.<sup>6,7</sup> Despite the growing interest in sc-CO<sub>2</sub> extraction for coffee pulp valorization, research on the bioaccessibility, bioavailability, and bioactivity of its bioactive compounds remains extremely limited.

<sup>a</sup>Department of Agricultural Chemistry and Food Science, Faculty of Science, C/ Francisco Tomás y Valiente, 7; Universidad Autónoma de Madrid, 28049 Madrid, Spain. E-mail: alicia.gil@uam.es, maria.martin@uam.es

<sup>b</sup>Department of Production and Characterization of Novel Foods, Institute of Food Science Research, CIAL (UAM-CSIC), 28049 Madrid, Spain



To accurately assess the potential health benefits of these extracts, it is crucial to evaluate their bioactivity under physiologically relevant conditions, as the human digestive system subjects ingested food into complex enzymatic breakdown and absorption processes that can significantly modify their bioavailability and efficacy. The harmonized *in vitro* simulated gastrointestinal digestion model (e.g., INFOGEST 2.0) is an indispensable tool for preliminary screening.<sup>8</sup> It predicts the metabolic fate of bioactive compounds through simulated sequential enzymatic and pH changes encountered during digestion, providing critical insights into bioaccessibility and potential health benefits of these compounds post-digestion, prior to *in vivo* studies.<sup>9</sup> Coupling *in vitro* digestion with *in vitro* models of the human intestinal epithelium cell layer, such as the Caco-2 monolayer, offers transport and permeability characteristics similar to those of human intestinal tissue, facilitating a deeper understanding of the bioavailability and metabolism of coffee pulp bioactive compounds in the human body.<sup>10</sup> Moreover, the development of advanced and sophisticated intestinal co-culture models better mimics the intestinal immune environment by incorporating epithelial-immune cell crosstalk, allowing for a more physiologically relevant investigation compared to traditional monoculture models. In this sense, co-cultures of Caco-2 cells with human-derived (Caco-2/THP-1) or murine-derived (Caco-2/RAW264.7) macrophage cell lines have been developed.<sup>11</sup> Specifically, the Caco-2/THP-1 co-culture is more insightful because it integrates a polarized human intestinal epithelial barrier with human macrophage-like immune cells, enabling evaluation of epithelial-immune communication in a fully human-specific interface. In contrast, RAW264.7 is a murine macrophage line and thus provides a cross-species model when paired with Caco-2 cells. This human relevance is advantageous for probing the potential health-related effects of bioactives, such as antioxidant and anti-inflammatory activities.<sup>12</sup> While sc-CO<sub>2</sub> extraction of coffee pulp has been studied, the post-digestion bioactivity in a human-relevant intestinal-immune co-culture model remains unexplored.

Chronic diseases, including neurodegenerative disorders and cardiovascular diseases, are often associated with chronic inflammation and oxidative stress, and are among the leading causes of death worldwide. This underscores the urgent need for new preventative strategies, such as the use of dietary antioxidants and anti-inflammatory agents.<sup>13</sup> Coffee pulp extracts, enriched with (poly)phenols and other bioactive compounds, hold therapeutic potential to exert antioxidant and anti-inflammatory effects by scavenging free radicals and suppressing pro-inflammatory cytokine production post-digestion. Previous studies have demonstrated that *in vitro* digested coffee pulp aqueous extracts exhibit hypolipidemic,<sup>14</sup> antimicrobial,<sup>15</sup> and antioxidant effects.<sup>16</sup> However, the bioactivity profile may differ significantly for EtOH-modified sc-CO<sub>2</sub> extracts, as the latter possess a distinct lipophilic matrix expected to enhance the retention of non-polar bioactive compounds (e.g., caffeine), potentially leading to superior anti-inflammatory and antioxidant properties after digestion.

Understanding the molecular basis underlying biological activity is essential for the rational development of functional compounds and therapeutic strategies. In recent years, the integration of experimental approaches with *in silico* analyses have emerged as a powerful tool to elucidate mechanisms of action, predict molecular interactions, and support biological observations.<sup>10</sup> To date, the specific health benefits of *in vitro* gastrointestinal digestion of coffee pulp sc-CO<sub>2</sub> extracts remain underexplored and require further investigation.

Consequently, given that EtOH-modified sc-CO<sub>2</sub> technology provides a sustainable and efficient approach for recovering bioactive compounds from coffee pulp, the integration of *in vitro* digestion with cell-based assays offers a realistic method to evaluate their bioavailability and potential health benefits. As oxidative stress and inflammation are major contributors to chronic diseases, this study aimed to unlock the therapeutic potential of an EtOH-modified sc-CO<sub>2</sub> coffee pulp extract. We provide a comprehensive profile of its bioactive compounds after digestion using the INFOGEST 2.0 protocol. Their antioxidant and anti-inflammatory activities were evaluated in a human intestinal co-culture model, while bioinformatic modeling provided a molecular rationale for the observed biological activities.

## 2. Materials and methods

### 2.1. Chemicals

HPLC-grade acetonitrile was obtained from PanReac AppliChem (Barcelona, Spain). 3-(4,5-Dimethylthiazol-2-yl)-5-(3-carboxymethoxyphenyl)-2-(4-sulfophenyl)-2H-tetrazolium (MTS) was acquired from Promega (Madison, WI, USA). Analytical standards (protocatechuic acid, chlorogenic acid, caffeine, and 7-ethoxycoumarin), phenazine methosulfate (PMS), lipopolysaccharides from *Escherichia coli* O111:B4, phorbol 12-myristate 13-acetate (PMA), pepsin from porcine gastric mucosa (P6887), pancreatin from porcine pancreas (P7545), lipase from porcine pancreas (L3126), bile extract porcine (B8631), Bradford reagent and bovine serum albumin (BSA) were purchased from Sigma Aldrich (Sigma-Aldrich, St Louis, MO). Rabbit gastric extract (RGE 15) was from Lipolytech (Marseille, France). Antibiotic-antimycotic solution and RPMI-1640 Medium were supplied by Corning (Manassas, USA). High-glucose Dulbecco's modified Eagle's medium (DMEM), trypsin 0.25% solution, and phosphate-buffered saline (PBS) were purchased from Cytiva (Utah, USA). Fetal bovine serum (FBS), non-essential amino acids (NEAAs), and Hanks' balanced salt solution (HBSS) were provided by Gibco (Paisley, UK). All remaining reagents are of analytical grade.

### 2.2. Coffee pulp flour and extracts preparation

Coffee pulp flour and extracts were prepared following previous findings.<sup>6</sup> Briefly, coffee pulp from *Coffea arabica* (sourced from "Las Morenitas", Nicaragua) was cryogenically ground using a laboratory mill (IKA, Germany) and sequentially sieved to obtain a 250–500 μm flour fraction. For the EtOH-modified



sc-CO<sub>2</sub> extraction, 50 g of this flour was processed in a supercritical fluid extraction system equipped with a 2 L extraction vessel (SF2000 model, Thar Technologies, USA) at 65 °C and 23 MPa, using 9% ethanol (w/w, relative to CO<sub>2</sub>) as a co-solvent at a constant CO<sub>2</sub> flow rate of 83 g min<sup>-1</sup> for 120 min. After extract collection *via* pressure drop, the extract was rotary-evaporated to dryness (IKA, Germany), and the resulting extract was stored at -20 °C. Conventional aqueous and ethanolic (96%, v/v) extractions were performed at a 1:24 (g mL<sup>-1</sup>) solid-to-liquid ratio, mirroring the ethanol-to-flour ratio in the supercritical process. Mixtures were stirred (65 °C, 120 min) and filtered (Whatman No. 1); subsequently, aqueous extracts were freeze-dried and ethanolic extracts were vacuum-dried, before their storage at -20 °C.

### 2.3. Static *in vitro* simulated gastrointestinal digestion

**2.3.1. Chemical composition of coffee pulp extract.** The composition of the food matrices dictates the selection of the appropriate digestion procedure. Accordingly, lipid content was determined using the Folch method, and protein content was quantified using the Bradford assay with a BSA calibration curve, with results expressed as mg g<sup>-1</sup> extract.<sup>17</sup> Total flavonoid content was measured by the aluminum chloride assay, and results were reported as mg catechin equivalents (CE) per g extract.<sup>7</sup> Total phenolic, caffeine, protocatechuic acid, and chlorogenic acid contents in the extracts were quantified in our previously published work,<sup>6</sup> following the methodologies detailed in sections 2.4 and 2.5.

**2.3.2. Optimization of *in vitro* digestion of coffee pulp extract.** To guarantee reproducibility of digestion and cell culture compatibility, the standard units of digestive enzyme activity and the bile salt concentration (Table S1) were determined as detailed in INFOGEST 2.0.<sup>8</sup> Additionally, the lipid content in the EtOH-modified sc-CO<sub>2</sub> extract (Table S2) was quantified to adjust the digestion parameters for a lipid-rich matrix by increasing pancreatic lipase activity.<sup>8</sup>

The digestion pool was adapted for cell experiments. Briefly, 1 mL of water was mixed with 1 mL of simulated salivary fluid containing oral saliva, and the mixture was incubated for 2 min at 37 °C with mixing (oral phase). For the gastric phase, the oral phase (2 mL) was combined with 2 mL simulated gastric fluid, achieving final pepsin and gastric lipase activities of 2093 and 60 U mL<sup>-1</sup>, respectively, by adding rabbit gastric extract solution, then adjusted to pH 3.0, and incubated 2 h at 37 °C under rotation. In the intestinal phase, the gastric phase (4 mL) was mixed with 4 mL simulated intestinal fluid containing bile salts (2.5–5 mM in digestion) and pancreatin powder (pancreatic lipase activity 500–2000 U mL<sup>-1</sup> in digestion), adjusted to pH 7.0, and incubated at 37 °C for 2 h under rotation. After centrifugation (2600g, 4 °C, 30 min), the supernatants (digesta) were collected and diluted (1:3–1:69 ratios, v/v) in complete DMEM medium with 10% FBS (section 2.8.1) to reduce bile salts and inactivate enzymes. Caco-2 cells were subsequently treated with different digesta to optimize the digestion pool (>85% viability, MTS method in section 2.8.2).<sup>18</sup> The >85% viability threshold was chosen to

claim non-cytotoxicity according to the International Organization for Standardization guidelines (ISO 10993-5:2009).

Sample loadings were screened under the optimized digestion pool. Varied amounts (10–160 mg, *i.e.*, 1.25–20 mg mL<sup>-1</sup> in the final pool) of EtOH-modified sc-CO<sub>2</sub> extracts were suspended in 1 mL of water and digested using the optimized bile salts and pancreatic lipase. Resulting digesta were diluted (1:9–1:49 ratios, v/v) in complete medium containing 10% FBS to treat Caco-2 cells, and sample loading and dilution factor were selected to achieve >85% cell viability (section 2.8.2). Absence of a floating lipid layer after centrifugation was recorded to confirm complete digestion. Finally, digesta of EtOH-modified sc-CO<sub>2</sub> extract (sc-CO<sub>2</sub>), water extract (water), ethanol extract (EtOH), or mixed standard compounds (StdMix; corresponding to the content of protocatechuic acid, chlorogenic acid, and caffeine in EtOH-modified sc-CO<sub>2</sub> extract) were prepared using optimized conditions.

### 2.4. Total phenolic content (TPC)

Diluted digesta (10 µL, 1:4 v/v dilution) and Folin–Ciocalteu reagent (150 µL, 1:14 v/v dilution) were mixed in a 96-well plate; after 3 min, 50 µL of 20% (w/v) Na<sub>2</sub>CO<sub>3</sub> was added. Following a 2.5 h incubation (room temperature), absorbance was recorded at 750 nm using a microplate reader (Biotek, USA). Results were calculated using a gallic acid standard curve and expressed as mg GAE mL<sup>-1</sup> of digesta.<sup>6</sup>

### 2.5. Identification and quantification of compounds by UPLC-MS

The identification and quantification of protocatechuic acid, chlorogenic acid, and caffeine were performed using an ACQUITY Arc LC System coupled to an ACQUITY QDa Mass Detector (UPLC-MS; Waters, USA) as described in our previous study.<sup>6</sup> Digesta were diluted 1:4 (v/v, in water) for protocatechuic acid and caffeine, and 1:1 (v/v, in water) for chlorogenic acid, then were syringe-filtered (0.45 µm) and spiked with 10 µg mL<sup>-1</sup> of the internal standard 7-ethoxycoumarin before injection.<sup>6</sup> Concentrations were obtained using the standard calibration curve and expressed as µg mL<sup>-1</sup> of digesta. The bioaccessibility of compounds during digestion was calculated as:

$$\text{Bioaccessibility (\%)} = \frac{C_{\text{digesta}} \times V_{\text{digesta}}}{C_{\text{extract}} \times m_{\text{extract}}} \times 100$$

where  $C_{\text{digesta}}$  and  $C_{\text{extract}}$  are the compound concentration in digesta (mg mL<sup>-1</sup>) and extract (mg g<sup>-1</sup>), respectively.  $V_{\text{digesta}}$  is the digesta volume (mL), and  $m_{\text{extract}}$  is the sample loadings (g). Relative bioaccessibility (%) was normalized against StdMix digesta.

### 2.6. ABTS free radical scavenging capacity

The ABTS<sup>+</sup> free radical stock solution was prepared by reacting 7 mM ABTS (20 mL) with 2.45 mM potassium persulfate (10 mL) overnight in the dark at room temperature. To ensure signal stability and minimize baseline drift, the working solu-



tion was prepared extemporaneously by diluting the stock solution in 5 mM PBS (pH 7.4) until a target absorbance of 0.70–0.80 at  $\lambda = 734$  nm was achieved. For the assay, 30  $\mu\text{L}$  of diluted digesta (1 : 99 v/v in water) was mixed with 270  $\mu\text{L}$  of working solution in a 96-well plate. After incubation for 10 min in the dark at room temperature, endpoint absorbance was measured at 734 nm using a microplate reader. Scavenging capacity was quantified using a Trolox calibration curve and expressed as  $\mu\text{g}$  Trolox equivalent (TE) per mL of digesta.<sup>6</sup>

### 2.7. *In vitro* 15-lipoxygenase (15-LOX) and cyclooxygenase 2 (COX-2) enzyme inhibition assay

Coffee pulp extracts (6.25 mg mL<sup>-1</sup>) and digesta (1 : 5 dilution, v/v) was prepared for 15-LOX inhibition assay using the Lipoxygenase Inhibitor Screening Assay Kit (Item No. 760700, Cayman Chemical, USA), while COX-2 inhibition was assessed at 0.3125 mg mL<sup>-1</sup> extract and 1 : 10 (v/v) diluted digesta using the COX-2 Inhibitor Screening Kit (Fluorometric) (ab283401, Abcam, UK). Nordihydroguaiaretic acid (NDGA) and celecoxib were included as positive controls for the 15-LOX and COX-2 assay, respectively. The procedure was performed according to the manufacturer's protocols, and results were expressed as a percentage of inhibition (%) as specified in the kit instructions.

### 2.8. Cell culture and viability test

**2.8.1. Caco-2 and THP-1 cell cultures.** Caco-2 cells (American Type Culture Collection, ATCC, USA) were cultured in high-glucose DMEM supplemented with 10% FBS, 1% non-essential amino acids, and 1% antibiotic–antimycotic solution at 37 °C with 5% (v/v) CO<sub>2</sub>. Medium was refreshed every two days, and cells were subcultured every 3–4 days at 60–70% confluence. THP-1 cells (ATCC, USA) were cultured in RPMI-1640 medium containing 10% FBS, 1% antibiotic–antimycotic solution, and 0.05 mM 2-mercaptoethanol at 37 °C under 5% (v/v) CO<sub>2</sub>. Once reaching  $8 \times 10^5$  cells per mL, cells were subcultured by centrifugation and were resuspended to  $2\text{--}4 \times 10^5$  cells per mL for the next passage. Passages 40–50 and 5–15 were used for Caco-2 and THP-1 cells, respectively.

**2.8.2. Caco-2 cell viability test.** Caco-2 cells were seeded in 96-well plates at  $5 \times 10^4$  cells per well (*i.e.*,  $1.5 \times 10^5$  cells per cm<sup>2</sup>). After 24 h, cells were washed with 100  $\mu\text{L}$  PBS and treated with 200  $\mu\text{L}$  digesta diluted in complete DMEM for 24 h. Medium was replaced with 100  $\mu\text{L}$  FBS-free DMEM, and 20  $\mu\text{L}$  MTS-PMS (333  $\mu\text{g}$  mL<sup>-1</sup> MTS and 25  $\mu\text{M}$  PMS) was added. After 4 h, absorbance was read at 490 nm using a microplate reader.<sup>6</sup> Cell viability was calculated relative to the control group treated with complete DMEM containing water.

**2.8.3. THP-1 cell viability test.** THP-1 cells ( $2.66 \times 10^5$  cells per mL) in complete RPMI medium containing 100 nM PMA (final DMSO < 0.1%) were seeded at  $2.66 \times 10^4$  cells per well in 96-well plates (*i.e.*,  $0.83 \times 10^5$  cells per cm<sup>2</sup>, 100  $\mu\text{L}$  per well) and differentiated for 72 h into macrophages (THP-1 m). Differentiation was confirmed by morphology and adhesion microscopically.<sup>12</sup> Cells were washed with PBS, rested 2 h in

complete RPMI without 2-mercaptoethanol, then treated with 100  $\mu\text{L}$  digesta diluted in complete RPMI without 2-mercaptoethanol for 24 h. Medium was replaced with 100  $\mu\text{L}$  FBS-free RPMI and 20  $\mu\text{L}$  MTS-PMS, incubated for 4 h, and read at 490 nm. Cell viability was calculated relative to the control group treated with complete RPMI containing water.

### 2.9. Evaluation of the cellular antioxidant activity (CAA) in Caco-2 cells

**2.9.1. Caco-2 cell viability test for CAA assay.** The Caco-2 viability assay followed section 2.8.2 with minor modifications to match CAA conditions. Cells were treated with 100  $\mu\text{L}$  digesta diluted in FBS-free DMEM for 1 h, instead of 200  $\mu\text{L}$  digesta diluted in complete DMEM for 24 h. The remaining procedures followed the methodology described in section 2.8.2. Cell viability was expressed relative to the control group treated with FBS-free containing water.

**2.9.2. CAA assay.** Caco-2 cells were seeded at  $5 \times 10^4$  cells per well in a 96-well black opaque plate and cultured for 24 h, then washed with 100  $\mu\text{L}$  PBS. Subsequently, 50  $\mu\text{L}$  FBS-free DMEM containing 7-ethoxycoumarin, 2',7'-dichlorofluorescein diacetate (DCFH-DA, 25  $\mu\text{M}$  in well), and 50  $\mu\text{L}$  of digesta diluted in FBS-free DMEM were added and incubated for 1 h. After PBS washing, cells were treated with 100  $\mu\text{L}$  HBSS containing 500  $\mu\text{M}$  2,2'-azobis[2-amidinopropane]dihydrochloride (AAPH). Fluorescence (Ex 485 nm/Em 538 nm) was recorded every 5 min for 1.5 h at 37 °C with positive (DCFH-DA + AAPH) and negative (DCFH-DA without AAPH) controls. Results were quantified by area under the curve and calculated as follow:<sup>19</sup>

$$\text{CAA unit (\%)} = \frac{\text{AUC}_{\text{Positive control}} - \text{AUC}_{\text{Sample}}}{\text{AUC}_{\text{Positive control}}} \times 100$$

### 2.10. Evaluation of the cellular anti-inflammatory activity in Caco-2/THP-1 co-culture model

An *in vitro* co-culture model was established comprising Caco-2 monolayer and THP-1 macrophage (Fig. S1).

**2.10.1. Differentiation of Caco-2 cells.** Caco-2 cells ( $4.70 \times 10^5$  cells per mL) were seeded on the apical (AP) compartment of Corning Transwell inserts (Corning 3412, USA, 6 well-format, growth area: 4.67 cm<sup>2</sup>, pore size: 0.4  $\mu\text{m}$ ) at  $1.5 \times 10^5$  cells per cm<sup>2</sup> (*i.e.*,  $7 \times 10^5$  cells per well, 1.5 mL per well). The complete DMEM in the AP chamber was refreshed every other day for 21 days. The basolateral (BL) medium (2.6 mL) was gradually changed from complete DMEM to complete RPMI without 2-mercaptoethanol: days 0–7, 0% RPMI; days 7–11, 33.3%; days 11–14, 50%; days 14–18, 66.6%; days 18–21, 100%. After 21 days, the differentiated monolayer (dCaco-2) was ready for the co-culture model.<sup>12</sup> The trans-epithelial electrical resistance (TEER) was monitored for 21 days using a Volt-Ohm meter (EVOM3, World Precision Instruments, USA), and only monolayers >1500  $\Omega$  cm<sup>2</sup> were used. TEER was calculated as follows:

$$\text{TEER (\Omega cm}^2\text{)} = (R_t - R_0) \times S,$$

where  $R_t$  is the resistance ( $\Omega$ ) with cells at different times,  $R_0$  is



blank resistance without cells, and  $S$  is membrane area ( $4.67 \text{ cm}^2$ ).

**2.10.2. Differentiation of THP-1 cells to macrophages.** THP-1 cells ( $3.08 \times 10^5$  cells per mL) were seeded in 6-well plates at  $8 \times 10^5$  cells per well (*i.e.*,  $0.83 \times 10^5$  cells per  $\text{cm}^2$ , 2.6 mL per well) and differentiated with 100 nM PMA (final DMSO < 0.1%) for 72 h into macrophages (THP-1 m). Differentiation was confirmed by morphology and adhesion. Cells were washed with PBS, rested in 2.6 mL complete RPMI without 2-mercaptoethanol for 2 h, and used for the co-culture model.<sup>12</sup>

**2.10.3. Assembly of dCaco-2 and THP-1 m co-cultured model and sample treatment.** THP-1 m in a 6-well plate were stimulated with LPS ( $1 \mu\text{g mL}^{-1}$ , 2.6 mL; 4 h). Transwell inserts with dCaco-2 were placed onto LPS-stimulated THP-1 m to form an inflamed co-culture, and LPS was retained in the BL compartment. AP medium was replaced with 1.5 mL digesta diluted in complete DMEM. As controls, complete DMEM containing water was added to the AP compartment with LPS-stimulated (positive) or non-stimulated (negative) THP-1 m in the BL chamber. TEER was measured at 0 and 24 h and normalized to the positive control. After 24 h ( $37 \text{ }^\circ\text{C}$  and 5%  $\text{CO}_2$ ), BL medium was collected and stored at  $-80 \text{ }^\circ\text{C}$ .<sup>12</sup> To ensure cytosafety after 24 h of inflamed co-culture treatment, THP-1 m viability in the BL compartment was tested using the MTS method (section 2.8.3).

**2.10.4. Measurement of cytokine secretion.** The concentrations of TNF- $\alpha$ , IL-6, CCL2, IL-1 $\alpha$ , IL-1 $\beta$ , IL-1ra, and IL-10 in the basolateral medium were quantified using the Ella Automated Immunoassay System (Catalog #600-100, Bio-Techne, USA) with a microfluidics-based Simple Plex cartridge for enzyme-linked immunosorbent assay (ELISA). Samples were routed through microfluidic channels to bind target proteins, washed, and incubated with detection antibodies. Each sample was analyzed in duplicate, with two glass nanoreactors coated with capture antibodies per channel and quantified using manufacturer-calibrated standard curves. The sample was diluted 2–500 times to fit the curve ranges. Data was processed in Simple Plex Explorer 4.1.0.22 (Bio-Techne, USA) and reported as  $\text{pg mL}^{-1}$  or  $\text{ng mL}^{-1}$  of medium.

**2.10.5. Bioinformatic analysis.** The protein–protein interaction networks among measured cytokines were generated in STRING (<https://stringdb.org>) with the organism set to *Homo sapiens*, active interaction sources limited to Experiments, Databases, and Co-expression, and a medium confidence threshold (minimum required interaction score = 0.4). The differentially expressed cytokines (compared to the positive control) were subjected to enrichment analysis for biological processes (Gene Ontology terms) and Kyoto Encyclopedia of Genes and Genomes (KEGG) pathways using STRING's built-in statistics against the *Homo sapiens* STRING background, with significance defined as a false discovery rate (FDR) < 0.05. Redundancy among significant biological process terms were reduced using REVIGO ([revigo.irb.hr](http://revigo.irb.hr)) with default settings (semantic similarity = SimRel, resulting list = 0.7, species = *Homo sapiens*). Finally, to align with the Caco-2/THP-1 co-culture model, enriched results were curated to report inflammation-relevant terms, including epithelial-macrophage crosstalk.

## 2.11. Statistical analysis

Results were presented as mean  $\pm$  standard deviation ( $n = 3$ ) unless stated otherwise. Significance was assessed in SPSS 24 using one-way analysis of variance (ANOVA) with Tukey *post-hoc* test at  $p < 0.05$ . A *t*-test compared the relative TEER value between 0 h and 24 h. Principal component analysis (PCA), Pearson correlation, and hierarchical clustering analysis (HCA, Ward method, and Euclidean distance) were performed using Origin 2024. The principal component regression (PCR) was analyzed using XLSTAT 2024. All graphs were generated using GraphPad Prism 9.1.2 and Origin 2024.

## 3. Results and discussion

### 3.1. Adapting the *in vitro* digestion protocol

The scientific community broadly recognizes the INFOGEST 2.0 technique as a preliminary model for food digestion; however, it is essential to acknowledge certain limitations. The composition of the intestinal phase might cause Caco-2 cells to detach due to the presence of active enzymes (*e.g.*, trypsin), and bile salts are known to exert cytotoxic effects at recommended concentrations.<sup>18</sup> In contrast, food-derived compounds generated during digestion, in combination with the digestion pool, may potentially cause cell damage.<sup>18</sup> Additionally, achieving a homogeneous digesta is crucial to avoid undesirable digesta products with insoluble materials or multiple phases, as could occur when the lipid load in the digested matrix is high.<sup>8</sup> Consequently, a three-step assessment was implemented to adapt the digestion process of investigated samples for further bioactivity assays, *i.e.*, evaluating the method for enzyme activity inactivation, selecting the most suitable bile salt and enzymatic pool, and determining the optimal sample loading.

Due to the presence of  $\alpha_1$ -antitrypsin in FBS, dilution with complete culture medium appears to be the most straightforward and least destructive detoxification method compared to heat inactivation and the use of enzyme inhibitors.<sup>20</sup> The latter methods could destroy thermolabile compounds and interfere with Caco-2 brush border enzyme activity.<sup>18</sup> Preliminary experiments indicated that the digestion pool (5 mM bile salt + 1000 U  $\text{mL}^{-1}$  pancreatic lipase) detached cell when diluted 1:49 (v/v) in culture medium without supplemented FBS, resulting in a dramatic loss of the numbers of cells remaining adherent, viable, and metabolically active (cell viability < 20%, data not shown), while cells could survive (cell viability 90.3%, Fig. 1A) with the same digestion pool diluted 1:9 (v/v) in complete medium containing 10% FBS, confirming the enzyme-inactivating effect of the FBS. Moreover, as shown in Fig. 1A, the increase in pancreatic lipase activity in the digesta significantly led to Caco-2 cell detachment, likely due to the presence of trypsin in the porcine pancreatin added to achieve the desired lipase enzymatic units. Conversely, a contrary outcome was observed in bile salt concentration, demonstrating reduced cytotoxicity under the same pancreatic lipase activity. A plausible reason is that specific components



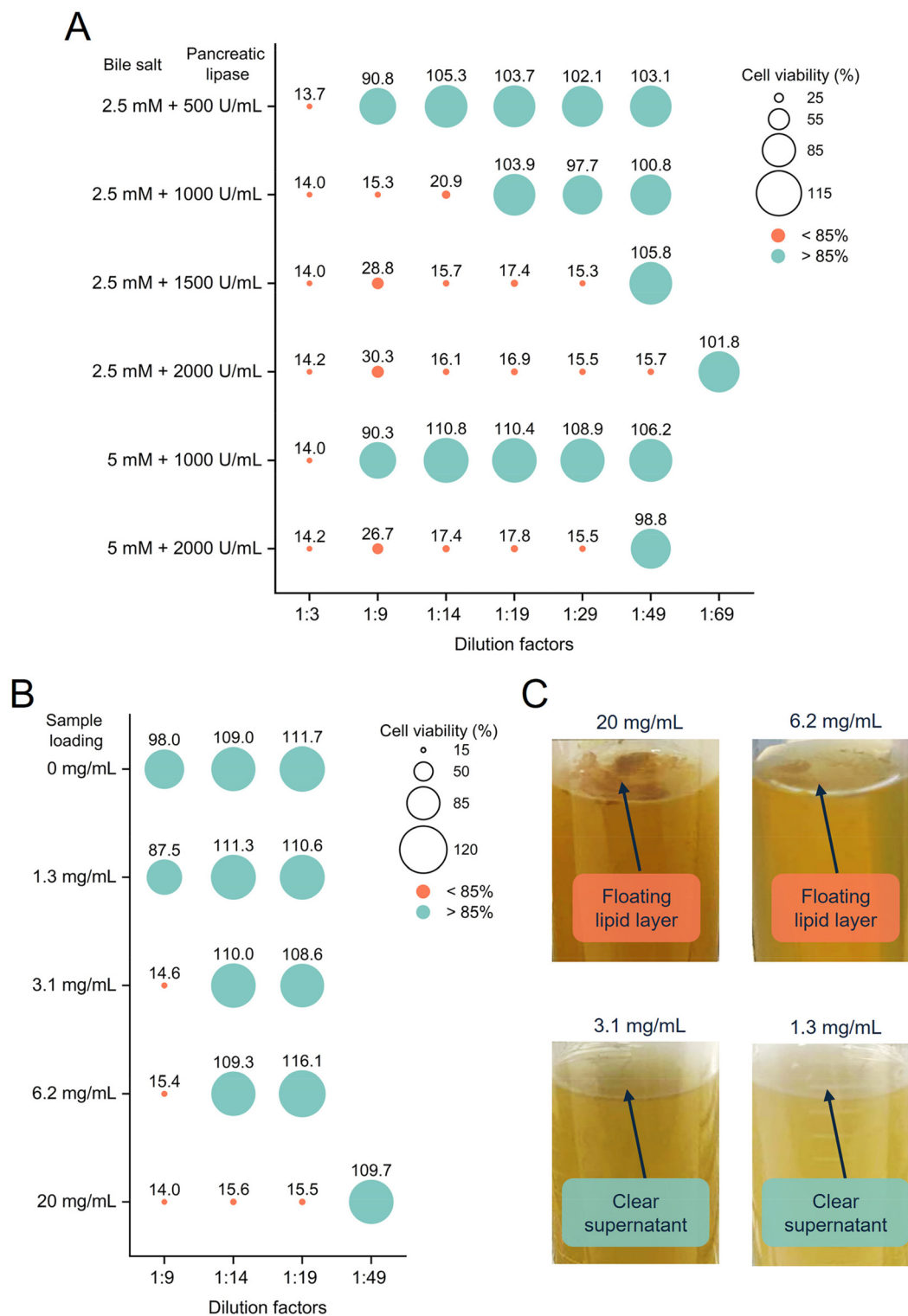


**Fig. 1** Optimization of sample loading, bile salt concentration and pancreatic lipase activity in *in vitro* simulated gastrointestinal digestion for subsequent cellular model: (A) Caco-2 cell viability (%) in monoculture treated with digestion pool using different bile salt concentration (2.5–5 mM) and pancreatic lipase (500–2000 U mL<sup>-1</sup>); (B) Caco-2 cell viability (%) in monoculture treated with digesta using different EtOH-modified sc-CO<sub>2</sub> extract concentrations (0–20 mg mL<sup>-1</sup>) at optimal digestion pool (5 mM bile salt and 1000 U mL<sup>-1</sup> pancreatic lipase); and (C) digestive interface behavior showing the presence of floating lipid layer after centrifugation. Results are expressed as the mean ± standard deviation (SD) of three independent replicates (*n* = 3).



in bile extract, such as phospholipids (*e.g.*, lecithin), cholesterol, and proteins, may interact with digestive enzymes, thereby reducing trypsin activity and obstructing cell detachment.<sup>18</sup> To more accurately mimic physiological concentrations following INFOGEST 2.0, the final digestion pool was adjusted to a bile salt concentration of 5 mM and a lipase activity of 1000 U mL<sup>-1</sup>, which enabled detoxification at a minimal initial dilution of 1:9 (*v/v*) with complete DMEM medium containing 10% FBS. Subsequently, to determine the appropriate sample loading, several sc-CO<sub>2</sub> extract concentrations were tested under the selected digestion pool. As depicted in Fig. 1B, elevated sample concentrations induced cytotoxicity in Caco-2 cells. A concentration of 6.2 mg mL<sup>-1</sup> could be recommended for dilution at a 1:14 (*v/v*) ratio. However, the latest was overloaded and led to incomplete lipid digestion, as evidenced by the formation of a floating lipid layer (Fig. 1C). Therefore, the final sample concentration was tuned to 3.1 mg mL<sup>-1</sup>, ensuring complete digestion without a floating layer while maximizing the concentration of bioactive compounds.

Summarizing, the selected conditions for preparing the EtOH-modified sc-CO<sub>2</sub> extract digesta were established at sample concentration of 3.1 mg mL<sup>-1</sup> (sample loading of 25 mg for 8 mL digestion volume), bile salt concentration of 5 mM and pancreatic lipase activity of 1000 U mL<sup>-1</sup>, which should be diluted in complete medium containing 10% FBS at 1:14 ratio (*v/v*) for cytosafe subsequent Caco-2 studies. To ensure experimental consistency and minimize potential artifacts from digestive enzymes or bile salts, all extracts were processed under standardized INFOGEST 2.0 conditions and applied to cells at an optimized 1:14 (*v/v*) dilution. This high dilution ratio has been shown to improve biocompatibility in intestinal models. Furthermore, since the digestive matrix was identical for all samples, the study focuses on the relative bioactivity of the digested compounds derived from different coffee pulp extracts.

### 3.2. Digestion-driven modulation of phenolic compounds and caffeine bioaccessibility

As shown in Fig. 2A, the TPC of the digesta varied significantly ( $p < 0.05$ ), with the water digesta exhibiting the highest value (727.3 μg GAE mL<sup>-1</sup>), followed by the sc-CO<sub>2</sub> digesta (675.3 μg GAE mL<sup>-1</sup>) and the EtOH digesta (642.4 μg GAE mL<sup>-1</sup>). These results aligned with our previous report on TPC in coffee pulp extracts (Table S2), where the water extract demonstrated a significantly higher TPC compared to the sc-CO<sub>2</sub> and EtOH extracts. This could be due to water's higher polarity, which enhanced the solubilization of additional hydroxyl-containing phenolics, leading to an increased TPC determined by the Folin–Ciocalteu method.<sup>6</sup> The sc-CO<sub>2</sub> digesta demonstrated a markedly elevated TPC compared to StdMix digesta, potentially attributable to the presence of additional phenolics, such as gallic acid and caffeic acid, in the sc-CO<sub>2</sub> extracts,<sup>6</sup> as well as the significant presence of other substances, including proteins (Table S2) or protein derivatives resulting from gastrointestinal digestion hydrolysis, which may interact with the

Folin–Ciocalteu reagent, leading to an overestimation of TPC values. The bioaccessibility of TPC (Fig. 2A) was lower in all coffee pulp extract digesta than in the StdMix digesta. This was aligned with previous reports that proteins could entrap and precipitate phenolics,<sup>21</sup> forming insoluble complexes with (poly)phenols, which limited their diffusion in the analyzed supernatant and left them in the pellet, thereby reducing their apparent bioaccessibility.<sup>22,23</sup> Moreover, two targeted phenolic compounds (*i.e.*, protocatechuic and chlorogenic acids) were further identified and quantified by LC-MS. As depicted in Fig. 2B, protocatechuic acid was notably ( $p < 0.05$ ) more abundant in the sc-CO<sub>2</sub> digesta (61.2 μg mL<sup>-1</sup>) compared to the water (31.4 μg mL<sup>-1</sup>) and EtOH digesta (25.4 μg mL<sup>-1</sup>), which was attributed to the less-polar and the high-pressure extraction environment. In contrast, chlorogenic acid, which is more polar, exhibited significantly higher ( $p < 0.05$ ) concentrations in the water (25.3 μg mL<sup>-1</sup>) and EtOH (24.1 μg mL<sup>-1</sup>) digesta compared to sc-CO<sub>2</sub> digesta (Fig. 2C). The content of both protocatechuic and chlorogenic acids in the sc-CO<sub>2</sub> digesta was significantly ( $p < 0.05$ ) higher than that in StdMix digesta, suggesting that these two compounds in sc-CO<sub>2</sub> extract had a greater retention and stability than a mixture of pure standards during digestion. The bioaccessibility of protocatechuic acid was elevated across all extract digesta compared to the StdMix digesta (Fig. 2B). This might reflect the presence of anthocyanins and other phenolics derived from coffee pulp<sup>24</sup> that would be degraded or de-esterified under digestion conditions to yield protocatechuic acid.<sup>25</sup> The water extract showed the most significant increase (173.8%), compatible with its higher co-extraction of phenolic conjugates (as indicated by higher TPC, Table S2) that could serve as protocatechuic acid precursors. Divergent behavior was observed in chlorogenic acid bioaccessibility, displaying an increase for the sc-CO<sub>2</sub> digesta (143.6%) but sharp losses for the water (23.2%) and EtOH (27.2%) digesta (Fig. 2C). This might be attributed to the high lipid content in the sc-CO<sub>2</sub> extract (Table S2), which could favor the incorporation of chlorogenic acid into bile salt-lipid mixed micelles and provide hydrophobic microenvironments or inclusion complexes, thereby shielding oxidation, hydrolysis, and degradation, while also avoiding fiber/protein-driven precipitation losses during the digestion process.<sup>26</sup>

Although pure caffeine is regarded as stable and bioaccessible during simulated gastrointestinal digestion, a high caffeine concentration does not necessarily translate into high bioaccessibility due to the complex matrix of sc-CO<sub>2</sub> extract.<sup>10</sup> The caffeine content exhibited the most significant disparity across the digesta samples, with the sc-CO<sub>2</sub> digesta containing 287.6 μg mL<sup>-1</sup>, far exceeding the content in the EtOH and water digesta, which were 111.6 and 60.6 μg mL<sup>-1</sup>, respectively (Fig. 2D). This substantial difference highlighted the strong affinity of supercritical CO<sub>2</sub> for less polar molecules, such as caffeine. Contrary to the results found for protocatechuic and chlorogenic acids (Fig. 2B and C), the sc-CO<sub>2</sub> digesta exhibited a reduced caffeine concentration relative to the StdMix digesta (377.7 μg mL<sup>-1</sup>, Fig. 2D). Moreover, caffeine bioaccessibility



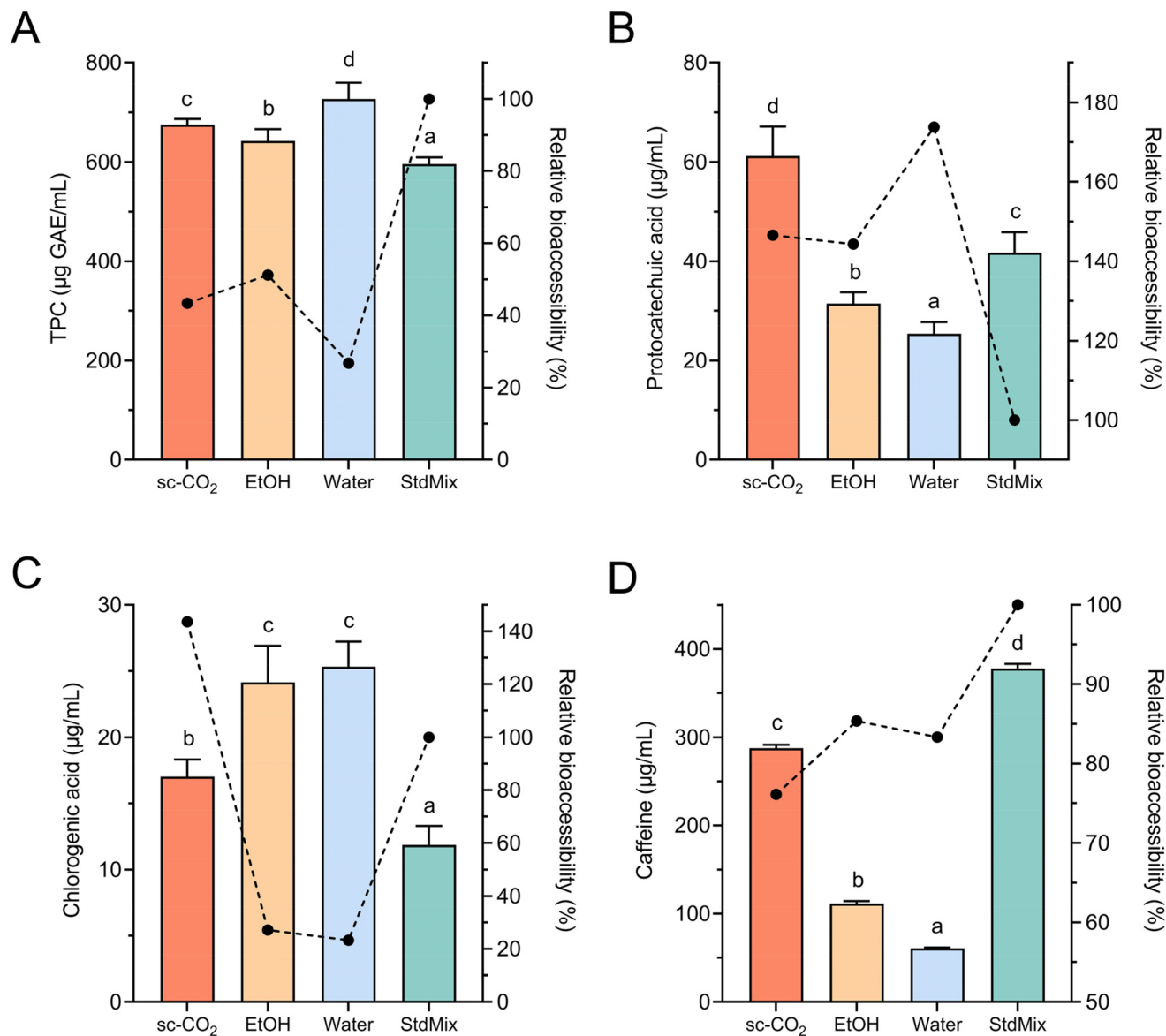


**Fig. 2** Characterization and relative bioaccessibility of the bioactive compounds in the digesta from different coffee pulp extracts: (A) total phenolic content; (B) protocatechuic acid; (C) chlorogenic acid; and (D) caffeine. Different letters indicate significant differences according to Tukey's test ( $p < 0.05$ ). Data are expressed as mean  $\pm$  SD ( $n = 3$ ). Bars represent compound contents (left y-axis), while dotted lines indicate relative bioaccessibility (right y-axis). GAE: gallic acid equivalent.

was consistently lower in all coffee pulp extract digesta (76.1%–85.4%) than in the StdMix digesta, with the sc-CO<sub>2</sub> digesta showing the lowest value (Fig. 2D), reflecting partial partitioning into the sedimented fraction or adsorption to solids rather than chemical degradation. Although caffeine is chemically stable and typically highly bioaccessible,<sup>10</sup> the lipid-rich sc-CO<sub>2</sub> extract matrix could enhance caffeine's association with hydrophobic macromolecules (e.g., lipid/bile aggregates) due to its low polarity, thereby diminishing initial partitioning of caffeine into the aqueous supernatant, and explaining the lowest measured caffeine bioaccessibility in sc-CO<sub>2</sub> digesta.<sup>26</sup> This finding was consistent with prior work indicating that coffee pulp containing lipid exhibited a

reduced caffeine bioaccessibility compared to low-lipid coffee pulp aqueous extract during *in vitro* digestion.<sup>10</sup> However, coffee pulp compounds retained in the pellet, which are considered non-bioaccessible in this assay, may undergo biotransformation in the colonic phase after microbial action, potentially extending the physiological effects beyond the upper gastrointestinal tract.<sup>27</sup>

### 3.3. Chemical-based antioxidant and anti-inflammatory activities

The ABTS free radical scavenging capacity (Fig. 3A) showed similar values for water digesta, compared to sc-CO<sub>2</sub> digesta, i.e., 4126  $\mu\text{g TE mL}^{-1}$  and 4015  $\mu\text{g TE mL}^{-1}$ , respectively. In



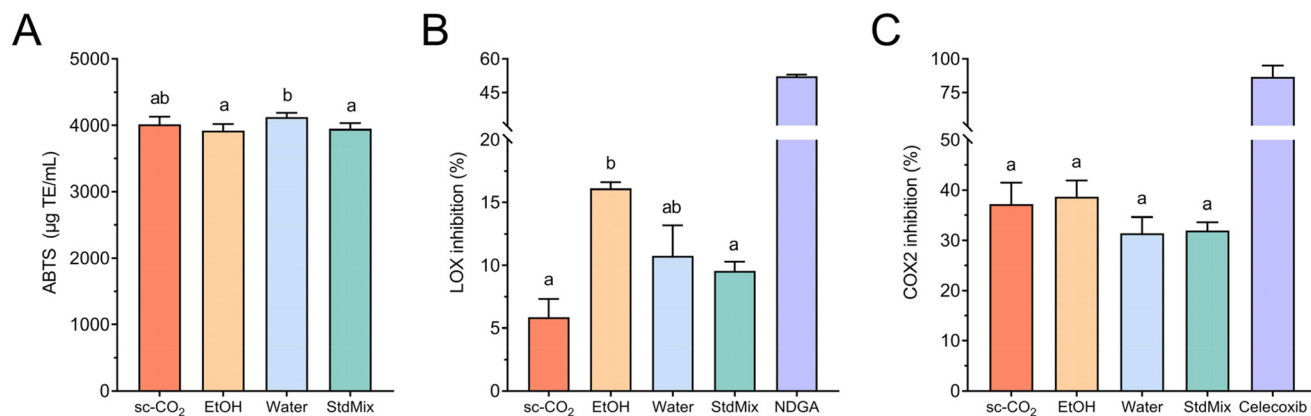


**Fig. 3** Chemical-based antioxidant and anti-inflammatory activities of the digests from different coffee pulp extracts: (A) ABTS free radical scavenging capacity ( $\mu\text{g TE mL}^{-1}$ ); (B) 15-lipoxygenase (LOX) inhibitory activity (%) of 5-fold diluted digests; and (C) cyclooxygenase 2 (COX2) inhibitory activity (%) of 10-fold diluted digests. Different letters indicate significant differences according to Tukey's test ( $p < 0.05$ ). Data are expressed as mean  $\pm$  SD ( $n = 3$ ). TE: Trolox equivalent; NDGA: nordihydroguaiaretic acid.

comparison, it was significantly higher ( $p < 0.05$ ) than StdMix ( $3949 \mu\text{g TE mL}^{-1}$ ) and EtOH ( $3923 \mu\text{g TE mL}^{-1}$ ) digests. This enhanced antioxidant activity might be attributed to superior solubility and the retention of more antioxidant compounds, such as (poly)phenols, in the water digesta during digestion compared to the sc-CO<sub>2</sub> or EtOH digests, as evidenced by the highest TPC of water digesta in Fig. 2A. This hypothesis aligned with the high coefficients ( $r = 0.89$  and  $1.49$  for Pearson correlation and PCR regression, respectively; Fig. 4) between TPC and ABTS, reinforcing the contribution of bioaccessible phenolics to antioxidant activity. Chlorogenic acid was identified as the primary phenolic compound contributing to ABTS scavenging ability, exhibiting a moderate positive Pearson correlation coefficient ( $r = 0.42$ , Fig. 4A), in contrast to the negative Pearson association observed with protocatechuic acid and caffeine. Additionally, the upward trend of the sc-CO<sub>2</sub> compared to StdMix digesta suggested that the presence and synergistic interactions of other polyphenols, proteins, or lipophilic compounds in the sc-CO<sub>2</sub> digesta might enhance its antioxidant activity.<sup>9</sup>

Lipoxygenase inhibition is closely associated with anti-inflammatory activity, as it reduces the synthesis of pro-inflammatory mediators. As shown in Fig. 3B, the quality control of a non-selective LOX inhibitor (NGDA) exhibited a robust inhibition (52.2%) at 100  $\mu\text{M}$ , confirming the expected performance of the chemical assay. Among the samples under study, the EtOH-digested samples demonstrated the highest LOX inhibition rate (16.1%). Although no statistical differences were observed between EtOH and water digesta, a distinct upward trend appears for the former. Conversely, these findings contradicted the TPC results (Fig. 2A) and antioxidant activity results (Fig. 3A), suggesting that ethanol was a more effective solvent for extracting potent anti-inflammatory substances, such as flavonoids and lipophilic compounds (Table S2), due to its intermediate polarity. Previous studies have indicated that the ethanolic extract of coffee pulp exhibits substantial LOX inhibitory activity, primarily attributed to

chlorogenic acid. The multiple hydroxyl groups in chlorogenic acid formed additional hydrogen bonds with LOX, resulting in a LOX-chlorogenic acid complex and enhancing the inhibitory effects on LOX enzymes.<sup>28</sup> This relationship was also experimentally confirmed in our study by the positive Pearson correlation ( $r = 0.57$ , Fig. 4A) and PCR regression ( $r = 0.71$ , Fig. 4B) found between chlorogenic acid content and LOX inhibitory activity. However, sc-CO<sub>2</sub> digesta exhibited the lowest LOX inhibition potential at 5.9%, which was less than the 9.6% observed for the StdMix digesta. This phenomenon may be due to the unique chemical profile of the sc-CO<sub>2</sub> extract, which is highly rich in fatty components (Table S2), that could be involved in the lipoxygenation reaction underlying the detection method. For instance, the presence of some fatty acids, such as the compound *cis,cis*-1,4-pentadiene system, identified in pure and EtOH-modified sc-CO<sub>2</sub> plant-derived extracts, could serve as substrates for lipoxygenase.<sup>29</sup> The presence of these substrates would produce more pro-inflammatory intermediate products (hydroperoxides) in the lipoxygenation reaction, which reduced the apparent LOX inhibition effectiveness of sc-CO<sub>2</sub> digesta. Therefore, LOX inhibition results in lipid-rich digesta should be interpreted as apparent LOX inhibition under the assay conditions.

Inhibition of COX-2 is a central anti-inflammatory strategy by limiting the synthesis of pro-inflammatory prostaglandins. Although no statistically significant differences were detected in the COX-2 inhibition rate (Fig. 3C) among all digests, the highest and lowest values were obtained for EtOH (38.7%) and water digesta (31.4%), respectively, implying that less-polar substances, such as protocatechuic acid, were mainly responsible for the COX-2 inhibitory activity.<sup>30</sup> This interpretation was further supported by the modest positive Pearson correlation ( $r = 0.36$ , Fig. 4A) and the highest PCR regression ( $r = 1.41$ , Fig. 4B) between protocatechuic acid and COX-2 inhibition rate. Notably, the inhibition rate of the sc-CO<sub>2</sub> digesta (37.2%) exceeded that of the StdMix digesta (32.0%), indicating that additional COX-2 inhibitor constituents present in the



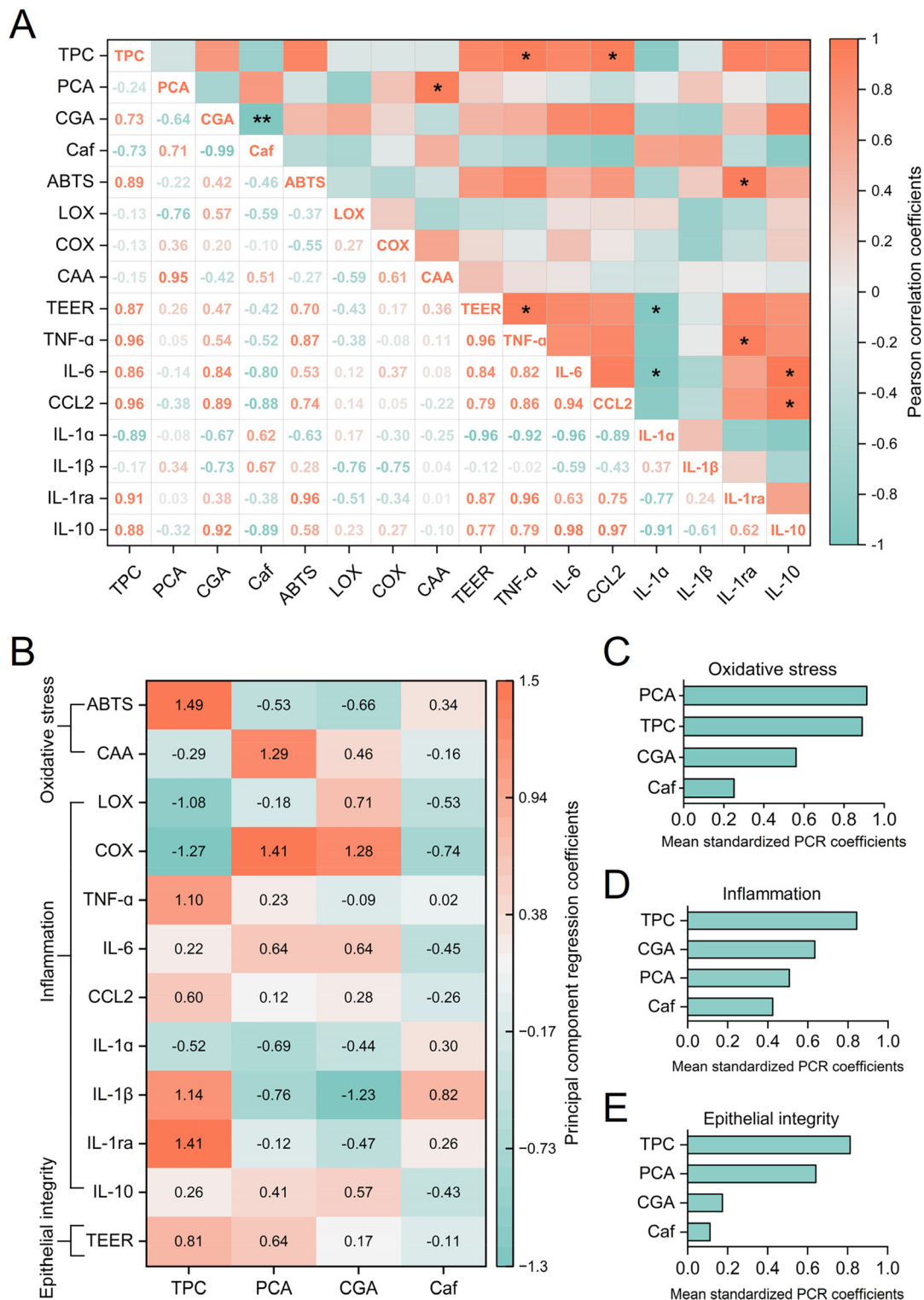


**Fig. 4** Heatmap of (A) Pearson correlation coefficients and (B) standardized principal component regression (PCR) coefficients between compounds and bioactivities. Mean standardized PCR coefficients for (C) oxidative stress; (D) inflammation; and (E) epithelial barrier integrity. \* Significantly correlated at  $p < 0.05$ ; \*\* significantly correlated at  $p < 0.01$ . TPC: total phenolic content; PCA: protocatechuic acid; CGA: chlorogenic acid; Caf: caffeine; ABTS: ABTS free radical scavenging capacity; LOX: 15-lipoxygenase inhibition activity; COX: cyclooxygenase 2 inhibition activity; CAA: cellular antioxidant activity; TEER: relative TEER value at 24 h.



sc-CO<sub>2</sub> extract remained sufficiently bioaccessible after digestion. This finding was consistent with prior reports that coffee extracts had superior COX-2 inhibitory activity compared to pure caffeine and chlorogenic acid, implicating other compounds, such as ferulic and quinic acids, and suggesting possible synergistic effects.<sup>31</sup>

Overall, these results preliminarily revealed the antioxidant and anti-inflammatory properties of coffee pulp sc-CO<sub>2</sub> extract digesta, demonstrating its capacity to neutralize free radicals and inhibit key inflammatory enzymes. However, chemical methods fail to capture the complexity of biological systems and cannot entirely replicate the physiological conditions in which these compounds exhibit their effects. To bridge this gap, additional cellular studies are necessary to gain a more profound understanding of the performance of these extracts in biologically relevant environments, elucidating their mechanisms of action, cellular uptake, and impacts on oxidative stress and inflammation at the molecular level.

### 3.4. Cellular antioxidant activity

Digesta compounds taken up and metabolized intracellularly could provide insights into cellular antioxidant activity. As shown in Fig. 5A, after treatment with a 1 : 14 dilution in FBS-free medium (final dilution of 1 : 29) for 1 h, cell viability was greater than 90% for all samples, confirming the suitability of this dilution for the CAA assay. The CAA results (Fig. 5B) revealed a non-significant trend ( $p > 0.05$ ) toward higher value for sc-CO<sub>2</sub> digesta (37.8%), followed by the EtOH digesta (34.0%) and the water digesta (32.0%), highlighting the advantage of sc-CO<sub>2</sub> extraction in preserving and retaining antioxidant components post-digestion. Notably, protocatechuic acid showed a significant Pearson correlation ( $r = 0.95$ ,  $p < 0.05$ , Fig. 4A) and the highest PCR regression ( $r = 1.29$ , Fig. 4B) with CAA, and the most significant mean PCR coefficients (Fig. 4C) to oxidative stress, underscoring that protocatechuic acid served as a potent antioxidant contributor to the intracellular antioxidant activity.<sup>32</sup> Previous studies have reported that protocatechuic acid can enhance the activity of endogenous antioxidant enzymes, such as glutathione peroxidase and superoxide dismutase, by activating cellular defense mechanisms, including the Nrf2 pathway, thereby providing protective effects against oxidative stress.<sup>33</sup> The higher CAA value of the sc-CO<sub>2</sub> digesta compared to the StdMix (33.7%) digesta suggested that the matrix complexity likely contained compounds that work synergistically to amplify cellular antioxidant effects. The lipid content in the sc-CO<sub>2</sub> extract (Table S2) undergoes enzymatic hydrolysis during digestion into lipophilic bioactives, such as fatty acid derivatives. These components integrate effectively into cell membranes' lipid bilayers, facilitating cellular uptake of other compounds and providing essential protection against peroxy radicals both at the membrane interface and intracellularly.<sup>34</sup>

### 3.5. Cellular anti-inflammatory activity

The development of the dCaco-2 and THP-1 m co-culture system provides a physiologically relevant model considering

intestinal barrier integrity and immune response. The morphology of THP-1 cells changed from round to elongated and flattened upon PMA induction, confirming their differentiation into THP-1 macrophages (Fig. S2). The viability of Caco-2 and THP-1 m cells in monoculture ranged from 113.9–120.9% (Fig. 5C) and 103.3–109.4% (Fig. 5F), respectively, after 24 h treatment with the digesta diluted with complete medium, suggesting that all digesta treatments did not exert cytotoxic effects but rather promoted cell proliferation and enhanced metabolic activity. The TEER values of Caco-2 monolayer development progressively increased from 4.9  $\Omega$  cm<sup>2</sup> on day 0 to a peak of 2782.4  $\Omega$  cm<sup>2</sup> on day 16, followed by a slight decline to 2446.7  $\Omega$  cm<sup>2</sup> on day 21 (Fig. 5D), demonstrating the formation of a tight and functional epithelial barrier, which was essential for assessing the interactions between digesta and the intestinal-immune interface.<sup>11</sup> All initial relative TEER values after digesta treatment at 0 h in the LPS-stimulated co-culture model ranged from 97% to 99% (Fig. 5E), indicating that digesta did not immediately disrupt barrier integrity.<sup>35</sup> Notably, relative TEER values significantly increased ( $p < 0.05$ ) within 24 h across all digesta treatments, with 106.1%, 103.2%, 105.5%, and 101.4% for sc-CO<sub>2</sub>, EtOH, water, and StdMix digesta, respectively (Fig. 5E). The restoration of relative TEER values suggested that digesta components, especially TPC ( $r = 0.87$  and  $0.81$  for Pearson correlation and PCR regression, Fig. 4), mainly contributed to epithelial resilience and tight junction reinforcement (Fig. 4E), possibly due to reduced inflammation-induced permeability changes. Among all digesta, the StdMix digesta displayed a significantly ( $p < 0.05$ ) lower relative TEER value after 24 h, which might be attributed to the adverse effects of higher caffeine content (Fig. 2D,  $r = -0.42$  and  $-0.11$  for Pearson correlation and PCR regression in Fig. 4), as caffeine was reported to influence barrier integrity *via* adenosine receptor signaling.<sup>36</sup> Additionally, the viability of THP-1m cells in the LPS-stimulated co-culture remained above 100% (Fig. 5G) following 24 h digesta treatment, confirming that these digesta did not trigger toxicity in the inflamed co-culture model. Overall, the observed changes in cell viability and TEER validated the successful establishment of the co-culture model. The differential effects of various digesta on intestinal and immune cell interactions underscored the need for further cytokine analysis to elucidate their anti-inflammatory activity.

As illustrated in Fig. 6, the significantly ( $p < 0.05$ ) higher levels of pro-inflammatory cytokines (TNF- $\alpha$ , IL-6, IL-1 $\alpha$ , and IL-1 $\beta$ ) and upregulation of chemokines (CCL2) in the LPS-stimulated positive control group compared to the non-LPS-stimulated negative control group confirmed the successful induction of an inflammatory response in the co-culture model. In contrast, the concurrent elevation of anti-inflammatory cytokines (IL-10 and IL-1ra) in the positive control represented a compensatory regulatory mechanism attempting to control excessive inflammation and restore immune homeostasis.<sup>37</sup> The protein-protein interaction network of all measured cytokines demonstrated their strong interconnectivity, which showed that cytokine proteins jointly contributed to the



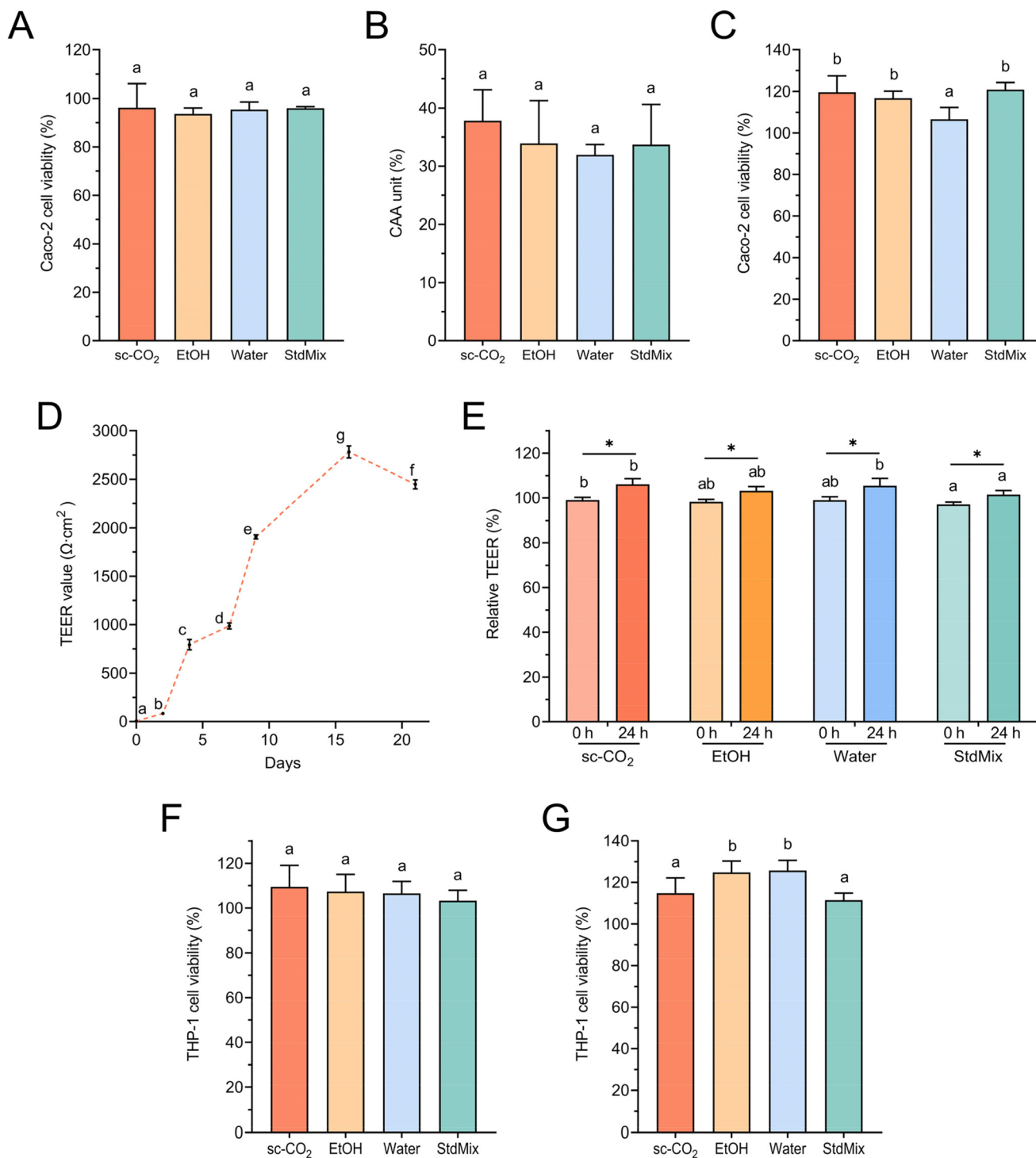


**Fig. 5** Cellular antioxidant activity of the digesta from different coffee pulp extracts in Caco-2 cells: (A) Caco-2 cell viability (%) treated with digesta diluted at a 1 : 14 ratio (v/v) in FBS-free medium for 1 h, and (B) CAA unit (%). Establishment of Caco-2/THP-1 co-culture model treated with digesta: (C) Caco-2 cell viability (%) in monoculture treated with digesta diluted at a 1 : 14 ratio (v/v) in complete medium for 24 h; (D) TEER values ( $\Omega \text{ cm}^2$ ) of Caco-2 monolayer development in Transwell during 21 days; (E) relative TEER value (%) normalized against positive control at 0 h and 24 h after sample exposure in Caco-2/THP-1 co-culture model; (F) THP-1 macrophage cell viability (%) in monoculture treated with digesta diluted at a 1 : 14 ratio (v/v) in complete medium for 24 h; and (G) THP-1 macrophage cell viability (%) in basolateral compartment of Caco-2/THP-1 co-culture model after 24 h sample exposure. Different letters indicate significant differences by the Tukey test ( $p < 0.05$ ). \* Significant differences between the relative TEER value of 0 h and 24 h by  $t$ -test ( $p < 0.05$ ). Results are expressed as mean  $\pm$  SD ( $n = 3$ ). CAA: cellular antioxidant activity; TEER: transepithelial electrical resistance.



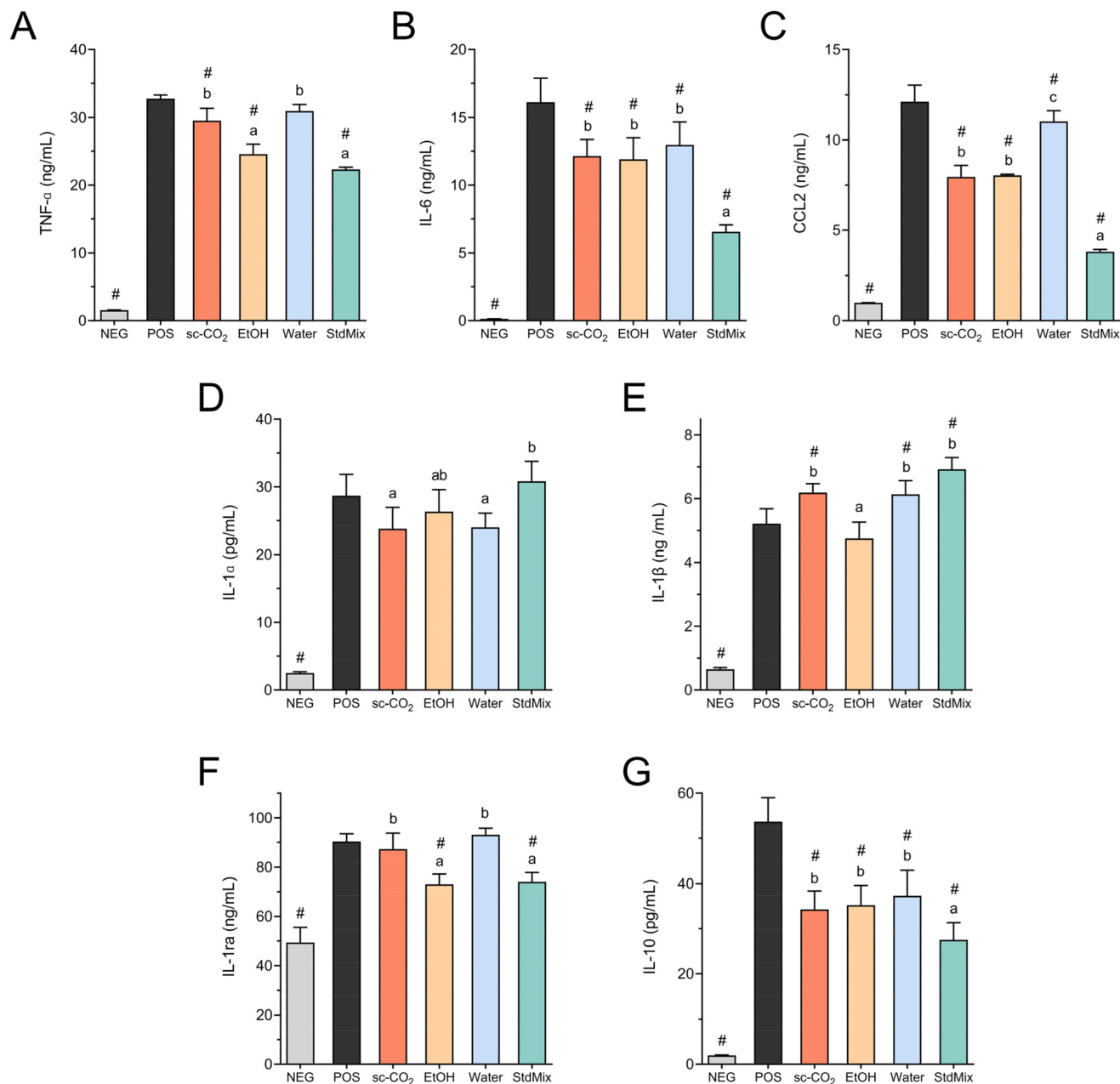


**Fig. 6** Effects of digesta from different coffee pulp extracts on cytokine contents in basolateral medium of Caco-2/THP-1 co-culture model: (A) TNF- $\alpha$ ; (B) IL-6; (C) CCL2; (D) IL-1 $\alpha$ ; (E) IL-1 $\beta$ ; (F) IL-1ra; and (G) IL-10. Different letters indicate significant differences within digesta groups according to Tukey's test ( $p < 0.05$ ). # indicates significant differences compared to the positive control group by Dunnett's test. POS: positive control with LPS stimulation; NEG: negative control without LPS stimulation.

shared functions (Fig. 7A). Furthermore, all cytokines in the digesta group exhibited significant changes ( $p < 0.05$ ) compared to the positive control group (Fig. 6), except for IL-1 $\alpha$  (Fig. 6D), indicating that these transepithelial fractions might alter cytokine homeostasis by influencing biological processes and signaling pathways, thereby exerting anti-inflammatory effects. Bioinformatic modeling allows the identification of relevant molecular targets and pathways, providing mechanistic insight into experimentally observed effects. In this regard, enrichment analysis of biological processes and pathways was

performed for each digesta group using the significantly altered cytokines identified for each group relative to the positive control (Table S3). In contrast, the universal panel of significantly enriched biological processes and pathways (Fig. 7B) was identified using cytokines that were significantly altered across all digesta groups (TNF- $\alpha$ , IL-6, IL-1 $\beta$ , CCL2, IL-1ra, and IL-10). As shown in Fig. 7B, biological process terms were curated to highlight inflammatory response to LPS, cytokine/chemokine production, and NF- $\kappa$ B/MAPK/JAK-STAT signaling, and epithelial-macrophage crosstalk in the Caco-2/THP-1



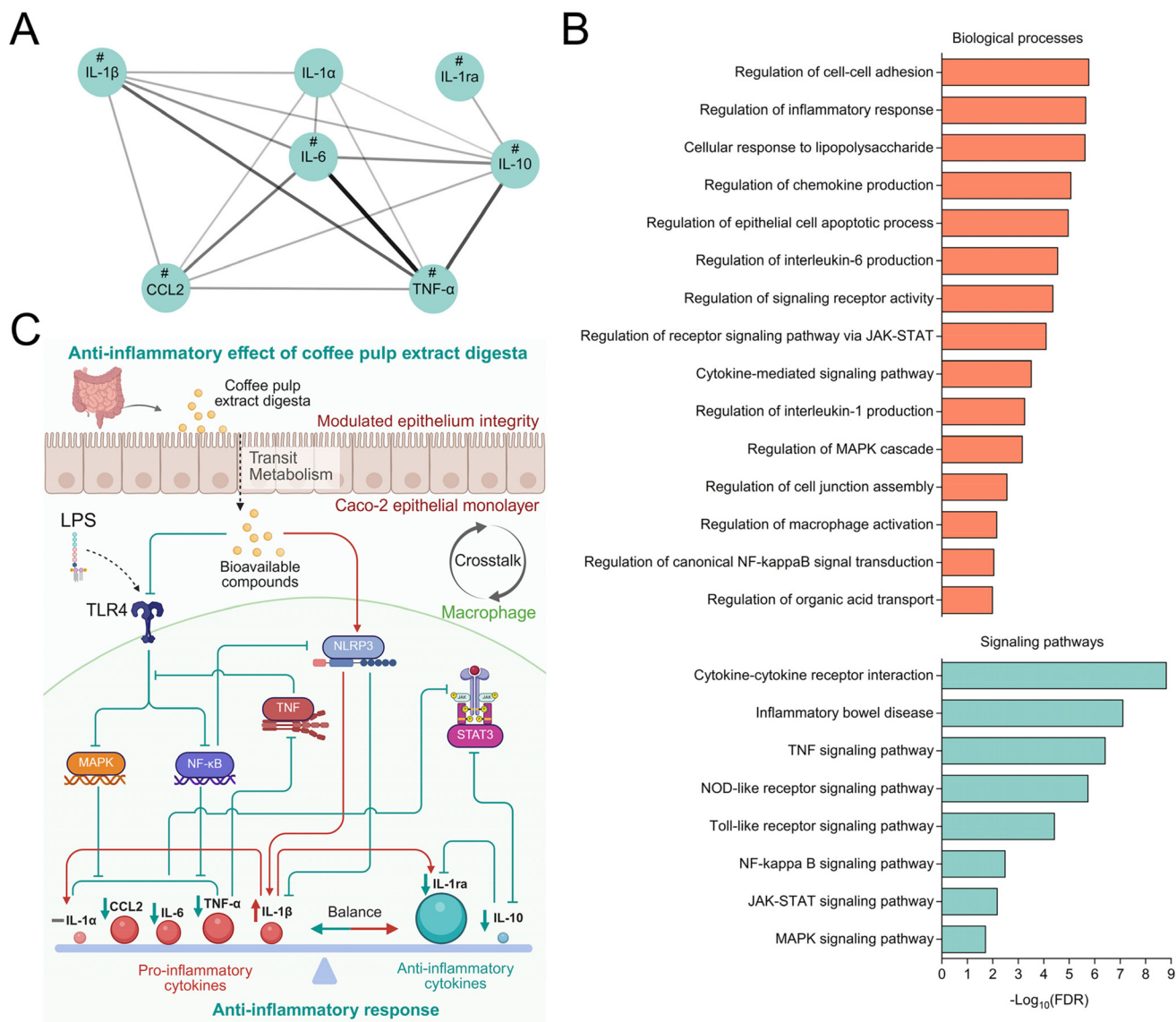


**Fig. 7** Cytokine profiling and mechanistic insights: (A) protein–protein interaction (PPI) network of measured cytokines; (B) enrichment analysis of significantly ( $p < 0.05$ ) modulated biological processes and signaling pathways based on differentially expressed cytokines ( $\# p < 0.05$ ) of digesta group compared to positive control; and (C) schematic representation of the anti-inflammatory effects of digesta in the Caco-2/THP-1 co-culture model. The line thickness and transparency of the network indicate the strength of data support. LPS: lipopolysaccharide.

Transwell model, including epithelial cell apoptosis, tight junctions, and organic acid transport. Signaling pathways further revealed underlying mechanisms, involving the modulation of TNF, NOD-like receptor (NLRP3), Toll-like receptor (TLR4), NF- $\kappa$ B, JAK-STAT (STAT3), and MAPK signaling pathways. This bioinformatics collectively painted a picture (Fig. 7C) of the potential framework in which coffee pulp extracts mitigate inflammatory disease.

TNF- $\alpha$ , IL-6, and CCL2, key cytokines involved in the NF- $\kappa$ B and MAPK pathways that stimulate and amplify inflammation in TLR4-activated macrophages (Fig. 7C), were decreased after digesta treatment compared to the positive control group (Fig. 6). As depicted in Fig. 6A, EtOH digesta (24.6 ng mL<sup>-1</sup>) and StdMix digesta (22.3 ng mL<sup>-1</sup>) exhibited the most signifi-

cant reductions in TNF- $\alpha$  levels, exhibiting stronger immunomodulatory effects than sc-CO<sub>2</sub> (29.5 ng mL<sup>-1</sup>) and water digesta (31.0 ng mL<sup>-1</sup>). A similar trend was observed for IL-6 levels (Fig. 6B), with StdMix digesta (6.5 ng mL<sup>-1</sup>) showing significantly lower levels ( $p < 0.05$ ) than sc-CO<sub>2</sub> (12.1 ng mL<sup>-1</sup>). At the same time, no differences were found among sc-CO<sub>2</sub>, EtOH, and water digesta. For CCL2, water digesta (11.0 ng mL<sup>-1</sup>) had significantly higher levels ( $p < 0.05$ ) than sc-CO<sub>2</sub> digesta (8.0 ng mL<sup>-1</sup>) and EtOH digesta (8.1 ng mL<sup>-1</sup>), while the StdMix digesta (3.8 ng mL<sup>-1</sup>) exhibited the most pronounced reduction in CCL2 expression (Fig. 6C). These results suggested that the sc-CO<sub>2</sub> and EtOH digesta were superior in modulating NF- $\kappa$ B- and MAPK-driven pro-inflammatory cytokines (Fig. 7C) than water digesta. In contrast, StdMix digesta



exhibited the most potent transepithelial anti-inflammatory effects. This may be attributed to the relatively higher TPC content in water digesta (Fig. 2B), as evidenced by the positive Pearson correlation and PCR regression (Fig. 4A and B) between TPC and these pro-inflammatory cytokines, as well as the high contribution of TPC to inflammation (Fig. 4C). Certain phenolic compounds enriched in water digesta, such as chlorogenic acid (Pearson correlation  $r = 0.54, 0.84, 0.89$  for TNF- $\alpha$ , IL-6, and CCL2, respectively; Fig. 4A), might be metabolized into caffeic acid, which could induce reactive oxygen species (ROS) generation at higher concentrations, potentially elevating pro-inflammatory cytokines and triggering more aggressive inflammatory states. Previous studies have revealed biphasic effects of chlorogenic acid, which might exert anti-inflammatory effects at low doses but pro-inflammatory effects at high doses.<sup>38</sup> In contrast, these pro-inflammatory cytokines showed a negative correlation with caffeine (Pearson correlation  $r = -0.52, -0.80, \text{ and } -0.88$  for TNF- $\alpha$ , IL-6, and CCL2, respectively; Fig. 4A), suggesting that caffeine may act as an inhibitor of NF- $\kappa$ B and MAPK. It was reported that caffeine can inhibit NF- $\kappa$ B by inhibiting phosphodiesterase, elevating cyclic adenosine monophosphate (cAMP) levels, and activating protein kinase A (PKA), ultimately suppressing TNF- $\alpha$  and IL-6 production. This could also reduce CCL2 synthesis by inhibiting the binding of activator protein 1/NF- $\kappa$ B to chemokine promoters.<sup>39</sup>

The observed IL-1 $\alpha$  levels across all digesta-treated groups were not significantly different from those of the positive control (28.7 pg mL<sup>-1</sup>), which may be a consequence of enhanced activation of the NLRP3 pathway and simultaneously suppressed activation of the NF- $\kappa$ B and MAPK pathways, resulting in a counteraction of IL-1 $\alpha$  production (Fig. 7C). IL-1 $\alpha$  is a pro-inflammatory cytokine that is often passively released from damaged epithelial/macrophage cells, making it a marker of crosstalk for inflammatory signaling and epithelial integrity. The sc-CO<sub>2</sub> digesta showed the lowest IL-1 $\alpha$  levels (23.8 pg mL<sup>-1</sup>; Fig. 6D), suggesting a protective effect against biological processes associated with epithelial stress (Fig. 7B and C). This reduction was probably due to the presence of potent lipophilic antioxidants that neutralized ROS and protected the epithelial integrity, as indicated by the highest CAA value (Fig. 5B) and relative TEER value (Fig. 5E) of sc-CO<sub>2</sub> digesta.<sup>40</sup> However, the StdMix digesta elicited the higher IL-1 $\alpha$  secretion (30.8 pg mL<sup>-1</sup>) than sc-CO<sub>2</sub> digesta (Fig. 6D). This suggested that pure compounds in the StdMix digesta, potentially caffeine ( $r = 0.62$  and  $0.30$  for Pearson correlation and PCR regression, respectively; Fig. 4), might induce cellular stress in THP-1 macrophage or Caco-2 epithelial cells, leading to passive IL-1 $\alpha$  release. Similar effects of caffeine ( $r = 0.67$  and  $0.82$  for Pearson correlation and PCR regression, respectively; Fig. 4) were found in IL-1 $\beta$  (Fig. 6E), with the StdMix digesta exhibiting the highest IL-1 $\beta$  secretion (6.9 ng mL<sup>-1</sup>). It was reported that high doses of caffeine activated IL-1 $\beta$  secretion *via* NLRP3 inflammasome activation (Fig. 7C).<sup>41</sup> In contrast, the EtOH digesta exhibited lower IL-1 $\beta$  levels (4.8 ng mL<sup>-1</sup>) than other digesta, suggesting an ability to attenuate the

induction of inflammasome activity. This effect may be linked to its potent inhibition of LOX and COX activities (Pearson correlation  $r = -0.76$  and  $-0.75$ , respectively; Fig. 4A), which reduces the synthesis of inflammatory mediators and thereby inhibits IL-1 $\beta$  secretion.<sup>42</sup>

IL-1ra is a natural inhibitor of IL-1 signaling, acting as an anti-inflammatory mediator to counteract the pro-inflammatory effects of IL-1 $\beta$ . The IL-1ra level was reduced after digesta treatment compared to the positive control group, suggesting a combined regulatory mechanism involving the NLRP3 and STAT3 pathways (Fig. 7C). Notably, sc-CO<sub>2</sub> and water digesta induced the higher IL-1ra levels ( $p < 0.05$ ) than EtOH and StdMix digesta (Fig. 6F). This increase may stem from STAT3 activation by phenolic acids released during digestion, as evidenced by the higher Pearson correlation and PCR regression with TPC ( $r = 0.91$  and  $1.41$ , respectively; Fig. 4) and the highest contribution of TPC to inflammation (Fig. 4E). The IL-1ra/IL-1 $\beta$  ratio was a critical determinant of net inflammatory activity.<sup>43</sup> It was found that the IL-1ra/IL-1 $\beta$  ratio were 14.1, 15.4, and 15.2 for sc-CO<sub>2</sub>, EtOH and water digesta, respectively, compared to the 10.7 in the StdMix digesta, reinforcing the critical role of interactions and synergies with other bioactive compounds present in extract matrix, such as flavonoids, lipids (fatty acids) and proteins (peptides), in inflammation alleviation.<sup>20</sup> IL-10 is another key anti-inflammatory cytokine, which is secreted later through the STAT3 pathway and directly suppresses the expression of inflammatory mediators (Fig. 7C). As shown in Fig. 6G, digesta-treated groups presented significantly lower ( $p < 0.05$ ) IL-10 levels than the positive control group, which was in line with the IL-1ra result (Fig. 6F). This was attributed to the reduction of pro-inflammatory cytokine burden (TNF- $\alpha$ , IL-6, CCL2), such that less IL-10 was needed to restore balance, suggesting that the digesta already suppressed inflammation.<sup>37</sup> This phenomenon was reflected by highly positive Pearson correlations between IL-10 and TNF- $\alpha$ , IL-6, and CCL2 ( $r = 0.79, 0.96, \text{ and } 0.96$ , respectively; Fig. 4A). The StdMix digesta showed lower IL-10 production ( $p < 0.05$ ) compared to the coffee pulp extract digesta-treated groups (Fig. 6G), which may be due to the high caffeine content that effectively dampened NF- $\kappa$ B-driven signaling, thereby limiting the activation of the STAT3 pathway and reducing anti-inflammatory mediators in prolonged inflammation. Taken together, coffee pulp extracts digesta acted as a modulator of the cytokine network, selectively suppressing key pro-inflammatory signals (TNF- $\alpha$ , IL-6, and CCL2) while allowing a controlled level of inflammasome cytokines (IL-1 $\alpha/\beta$ ) and maintaining balanced anti-inflammatory responses (IL-10 and IL-1ra, Fig. 7C), highlighting its potential therapeutic role in managing inflammatory conditions.

### 3.6. Multivariate analysis of digesta profiles

The PCA results (explaining 82.1% of the variation; Fig. 8A) clearly visualized distinct patterns in digesta derived from different coffee pulp extracts. The sc-CO<sub>2</sub> digesta, positioned in the upper-right quadrant, exhibited a robust correlation with IL-1ra, TEER, ABTS, and CAA antioxidant assay, and pro-



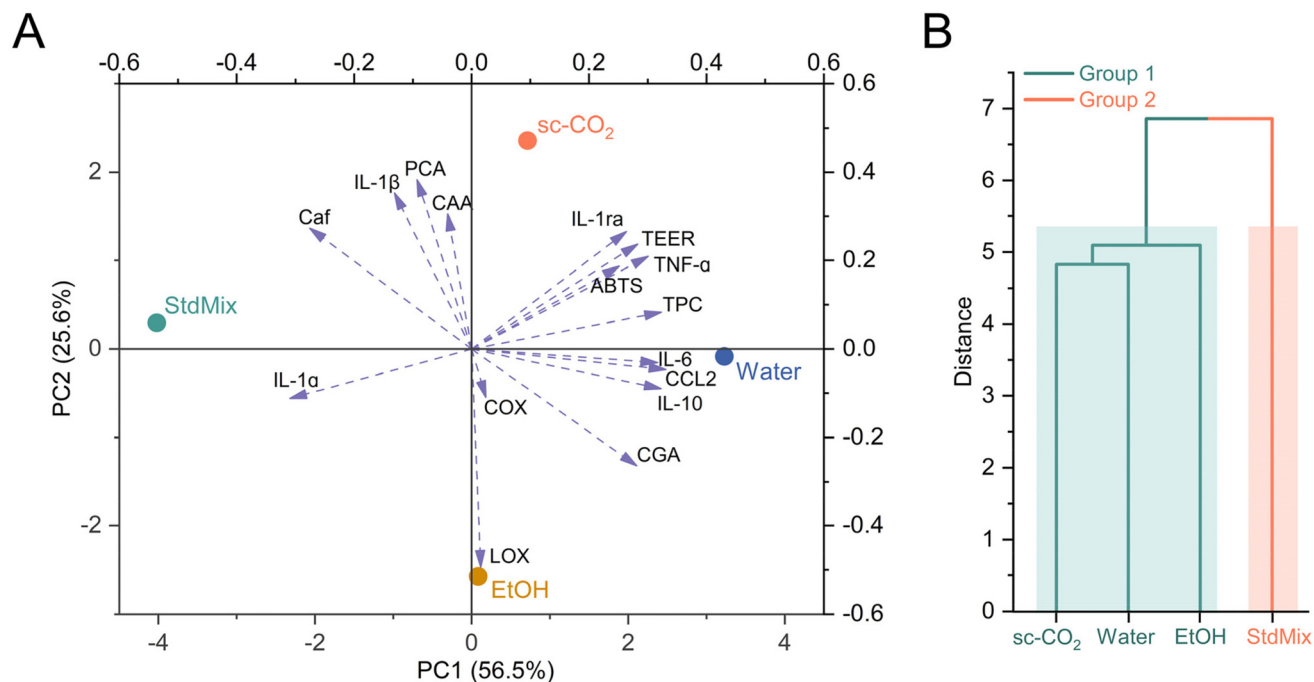


**Fig. 8** Exploratory data assessment including (A) principal component analysis biplot and (B) hierarchical clustering analysis for bioactive compounds and bioactivities of digesta from various coffee pulp extracts.

tocatechuic acid (Fig. 8A). These associations indicated that the sc-CO<sub>2</sub> digesta might enhance epithelial barrier integrity, scavenge free radicals and ROS, and upregulate IL-1ra, thereby exerting potent antioxidant and anti-inflammatory activities, likely due to its richness in protocatechuic acid. The water digesta was oriented along the positive X-axis, showing a close relationship with both pro-inflammatory (IL-6 and CCL2) and anti-inflammatory (IL-10) cytokines, as well as TPC (Fig. 8A). This dual response suggested that the water digesta had a balanced profile, capable of modulating inflammation through a combination of pro- and anti-inflammatory pathways. This effect might be related to the complexity of phenolic compounds in water digesta, as evidenced by its highest TPC (Fig. 2A). The EtOH digesta was situated in the lower-right quadrant and was closely aligned with the ability to inhibit LOX and COX. The specific positioning of the EtOH digesta highlighted its unique anti-inflammatory mechanism, namely enzymatic inhibition of inflammatory pathways, such as the arachidonic acid cascade, distinct from the cytokine-driven effects observed in sc-CO<sub>2</sub> and water digesta. Of note, StdMix digesta was the only sample placed in the negative Y-axis (Fig. 8A). This remarkable discrimination was also evidenced in the HCA analysis (Fig. 8B), with coffee pulp extracts digesta clustered into one group and separated from the StdMix digesta, highlighting the fundamental difference between simple mixtures of pure standard compounds and the complex compound interactions within extract matrices. The StdMix digesta was highly correlated with pro-inflammatory cytokines (IL-1 $\alpha$  and IL-1 $\beta$ ) but showed limited association

with anti-inflammatory cytokines (IL-1ra and IL-10), suggesting a lack of modulation in acute inflammatory responses.

While this study provides a robust platform for comparing the bioactivity of coffee pulp extracts, certain *in vitro* limitations apply. The static INFOGEST 2.0 model focuses on the upper gastrointestinal phase, thus excluding potential bio-transformation by colonic microbiota. Similarly, the Caco-2/THP-1 co-culture effectively models the epithelial-immune axis, although it simplifies the complex *in vivo* intestinal environment (*e.g.*, microbiota, mucus, circulation, and immune recruitment). Regarding the LOX inhibition assay, results should be interpreted considering the potential influence of the extract's lipid matrix. For future work, the hypothesis-generating pathway networks inferred from bioinformatics analysis need experimental confirmation to pin down the molecular mechanism definitively, and a comprehensive characterization of lipophilic compounds in the sc-CO<sub>2</sub> extract will help identify additional metabolites that may contribute to the observed activities.

## 4. Conclusion

This study demonstrated the potential of EtOH-modified sc-CO<sub>2</sub> extraction as an effective and sustainable strategy for valorizing coffee pulp, enriching it with gastrointestinal-bioaccessible compounds that possess antioxidant and anti-inflammatory properties. The EtOH-modified sc-CO<sub>2</sub> digesta exhibited a higher concentration of protocatechuic acid and caffeine



than water and EtOH digesta. The caffeine bioaccessibility of the EtOH-modified sc-CO<sub>2</sub> extract was lower than that of a pure-standard mixture, suggesting matrix-dependent trapping during digestion. This compositional advantage translated into stronger chemical and cellular antioxidant activity, as well as inhibition activities against 15-lipoxygenase and cyclooxygenase 2. In the Caco-2/THP-1 co-culture model, the EtOH-modified sc-CO<sub>2</sub> digesta attenuated NF- $\kappa$ B- and MAPK-associated inflammatory responses, particularly reducing IL-6 and CCL2, while maintaining epithelial integrity, effects predominantly attributed to the transepithelial metabolites derived from protocatechuic acid, chlorogenic acid, and caffeine. Notably, EtOH-modified sc-CO<sub>2</sub> digesta more effectively suppressed IL-1 $\alpha$  and increased anti-inflammatory cytokines (IL-10 and IL-1ra) compared to the standard mixture digesta, underscoring the importance of synergistic matrix interactions. This study provided compelling evidence for the promising application of coffee pulp-derived extracts as bioactive food ingredients and nutraceuticals for managing chronic diseases associated with oxidative stress and inflammation. Future studies on *in vivo* metabolism and compound-matrix interactions are warranted to validate the potential health benefits and translational relevance.

## Author contributions

Shuai Hu: data curation, formal analysis, investigation, methodology, software, writing – original draft. Miguel Rebollo-Hernanz: funding acquisition, software, writing – review & editing. María Martín-Trueba: methodology, software. Vanesa Benítez: funding acquisition, methodology, project administration. Yolanda Aguilera: methodology, software, visualization. María Ángeles Martín-Cabrejas: conceptualization, funding acquisition, resources, supervision, validation, writing – review & editing. Alicia Gil-Ramírez: conceptualization, funding acquisition, investigation, methodology, project administration, supervision, validation, writing – review & editing.

## Conflicts of interest

There are no conflicts to declare.

## Data availability

The data that support the findings of this study are available within the article and its supplementary information (SI). Supplementary information is available. See DOI: <https://doi.org/10.1039/d6fo00489j>.

## Acknowledgements

The results are part of the TED2021-129262A-I00 project, funded by MCIN/AEI/10.13039/501100011033 and by the

European Union “NextGenerationEU”/PRTR. This work was also supported by the project “Coffeeminds” (reference SI4/PJI/2024-00120), funded by the Community of Madrid through the direct grant agreement for the promotion of research and technology transfer at the Autonomous University of Madrid (UAM). SH is grateful to the China Scholarship Council (CSC) for awarding him a pre-doctoral fellowship (CSC 202208360052) to develop his Ph.D. at UAM.

## References

- 1 M. Ruesgas-Ramón, M. C. Figueroa-Espinoza, E. Durand, M. L. Suárez-Quiroz, O. González-Ríos, A. Rocher, G. Reversat, J. Vercauteren, C. Oger, J.-M. Galano, T. Durand and C. Vigor, Identification and quantification of phytoprostanes and phytofuran of coffee and cocoa by- and co-products, *Food Funct.*, 2019, **10**, 6882–6891, DOI: [10.1039/C9FO01528K](https://doi.org/10.1039/C9FO01528K).
- 2 S. Hu, A. Gil-Ramírez, M. Martín-Trueba, V. Benítez, Y. Aguilera and M. A. Martín-Cabrejas, Valorization of coffee pulp as bioactive food ingredient by sustainable extraction methodologies, *Curr. Res. Food Sci.*, 2023, **6**, 100475, DOI: [10.1016/j.crfs.2023.100475](https://doi.org/10.1016/j.crfs.2023.100475).
- 3 A. Gil-Ramírez, M. Rebollo-Hernanz, S. Cañas, I. Monedero Cobeta, P. Rodríguez-Rodríguez, A. Gila-Díaz, V. Benítez, S. M. Arribas, Y. Aguilera and M. A. Martín-Cabrejas, Unveiling the nutritional profile and safety of coffee pulp as a first step in its valorization strategy, *Foods*, 2024, **13**, 3006, DOI: [10.3390/foods13183006](https://doi.org/10.3390/foods13183006).
- 4 R. Romano, L. De Luca, G. Basile, C. Nitride, F. Pizzolongo and P. Masi, The use of carbon dioxide as a green approach to recover bioactive compounds from spent coffee grounds, *Foods*, 2023, **12**, 1958, DOI: [10.3390/foods12101958](https://doi.org/10.3390/foods12101958).
- 5 A. Vandepoosele, M. Draye, C. Piot and G. Chatel, Subcritical water and supercritical carbon dioxide: efficient and selective eco-compatible solvents for coffee and coffee by-products valorization, *Green Chem.*, 2020, **22**, 8544–8571, DOI: [10.1039/d0gc03146a](https://doi.org/10.1039/d0gc03146a).
- 6 S. Hu, M. Á. Martín-Cabrejas, D. M. Hernández, M. Martín-Trueba, S. Cañas, M. Rebollo-Hernanz, Y. Aguilera, V. Benítez and A. Gil-Ramírez, Tailored recovery of antioxidant fractions enriched in caffeine and phenolic compounds from coffee pulp using ethanol-modified supercritical carbon dioxide, *Food Res. Int.*, 2025, **200**, 115433, DOI: [10.1016/j.foodres.2024.115433](https://doi.org/10.1016/j.foodres.2024.115433).
- 7 L. Q. Thai, C. Niwat, S. Qin and N. Konsue, Supercritical carbon dioxide and ethanol-assisted extraction of bioactive compounds from bourbon, catimor, and caturra coffee pulp for maximized antioxidant and therapeutic properties, *Future Foods*, 2024, **9**, 100381, DOI: [10.1016/j.fufo.2024.100381](https://doi.org/10.1016/j.fufo.2024.100381).
- 8 A. Brodtkorb, L. Egger, M. Alminger, P. Alvito, R. Assunção, S. Ballance, T. Bohn, C. Bourlieu-Lacanal, R. Boutrou, F. Carrière, A. Clemente, M. Corredig, D. Dupont, C. Dufour, C. Edwards, M. Golding, S. Karakaya,



- B. Kirkhus, S. Le Feunteun, U. Lesmes, A. Macierzanka, A. R. Mackie, C. Martins, S. Marze, D. J. McClements, O. Ménard, M. Minekus, R. Portmann, C. N. Santos, I. Souchon, R. P. Singh, G. E. Vegarud, M. S. J. Wickham, W. Weitschies and I. Recio, INFOGEST static *in vitro* simulation of gastrointestinal food digestion, *Nat. Protoc.*, 2019, **14**, 991–1014, DOI: [10.1038/s41596-018-0119-1](https://doi.org/10.1038/s41596-018-0119-1).
- 9 S. Ketnawa, F. C. Reginio Jr., S. Thuengtung and Y. Ogawa, Changes in bioactive compounds and antioxidant activity of plant-based foods by gastrointestinal digestion: a review, *Crit. Rev. Food Sci. Nutr.*, 2022, **62**, 4684–4705, DOI: [10.1080/10408398.2021.1878100](https://doi.org/10.1080/10408398.2021.1878100).
- 10 S. Cañas, M. Rebollo-Hernanz, C. Braojos, V. Benítez, R. Ferreras-Charro, M. Dueñas, Y. Aguilera and M. A. Martín-Cabrejas, Understanding the gastrointestinal behavior of the coffee pulp phenolic compounds under simulated conditions, *Antioxidants*, 2022, **11**, 1818, DOI: [10.3390/antiox11091818](https://doi.org/10.3390/antiox11091818).
- 11 F. Guo, R. Tsao, C. Li, X. Wang, H. Zhang, L. Jiang, Y. Sun and H. Xiong, Polyphenol content of green pea (*Pisum sativum* L.) hull under *in vitro* digestion and effects of digestive products on anti-inflammatory activity and intestinal barrier in the Caco-2/RAW264.7 coculture model, *J. Agric. Food Chem.*, 2022, **70**, 3477–3488, DOI: [10.1021/acs.jafc.2c00102](https://doi.org/10.1021/acs.jafc.2c00102).
- 12 A. A. M. Kämpfer, P. Urbán, S. Gioria, N. Kanase, V. Stone and A. Kinsner-Ovaskainen, Development of an *in vitro* co-culture model to mimic the human intestine in healthy and diseased state, *Toxicol. In Vitro*, 2017, **45**, 31–43, DOI: [10.1016/j.tiv.2017.08.011](https://doi.org/10.1016/j.tiv.2017.08.011).
- 13 L. Xiao, Y. Sun and R. Tsao, Paradigm shift in phytochemicals research: evolution from antioxidant capacity to anti-inflammatory effect and to roles in gut health and metabolic syndrome, *J. Agric. Food Chem.*, 2022, **70**, 8551–8568, DOI: [10.1021/acs.jafc.2c02326](https://doi.org/10.1021/acs.jafc.2c02326).
- 14 C. Braojos, M. Rebollo-Hernanz, S. Cañas, Y. Aguilera, A. Gil-Ramírez, M. A. Martín-Cabrejas and V. Benítez, Coffee pulp simulated digestion enhances its *in vitro* ability to decrease emulsification and digestion of fats, and attenuates lipid accumulation in HepG2 cell model, *Curr. Res. Food Sci.*, 2024, **9**, 100804, DOI: [10.1016/j.crf.2024.100804](https://doi.org/10.1016/j.crf.2024.100804).
- 15 W. Khochapong, S. Ketnawa, Y. Ogawa and N. Punbusayakul, Effect of *in vitro* digestion on bioactive compounds, antioxidant and antimicrobial activities of coffee (*Coffea arabica* L.) pulp aqueous extract, *Food Chem.*, 2021, **348**, 129094, DOI: [10.1016/j.foodchem.2021.129094](https://doi.org/10.1016/j.foodchem.2021.129094).
- 16 S. Cañas, M. Rebollo-Hernanz, M. Martín-Trueba, C. Braojos, A. Gil-Ramírez, V. Benítez, M. A. Martín-Cabrejas and Y. Aguilera, Exploring the potential of phenolic compounds from the coffee pulp in preventing cellular oxidative stress after *in vitro* digestion, *Food Res. Int.*, 2023, **172**, 113116, DOI: [10.1016/j.foodres.2023.113116](https://doi.org/10.1016/j.foodres.2023.113116).
- 17 A. Shevel'yuhina, O. Babich, S. Sukhikh, S. Ivanova, E. Kashirskih, V. Smirnov, P. Michaud and E. Chupakhin, Antioxidant and antimicrobial activity of microalgae of the filinskaya bay (baltic sea), *Plants*, 2022, **11**, 2264, DOI: [10.3390/plants11172264](https://doi.org/10.3390/plants11172264).
- 18 A. Kondrashina, E. Arranz, A. Cilla, M. A. Faria, M. Santos-Hernández, B. Miralles, N. Hashemi, M. K. Rasmussen, J. F. Young, R. Barberá, G. Mamone, L. Tomás-Cobos, S. Bastiaan-Net, M. Corredig and L. Giblin, Coupling *in vitro* food digestion with *in vitro* epithelial absorption; recommendations for biocompatibility, *Crit. Rev. Food Sci. Nutr.*, 2023, **64**, 9618–9636, DOI: [10.1080/10408398.2023.2214628](https://doi.org/10.1080/10408398.2023.2214628).
- 19 M. E. Kellett, P. Greenspan and R. B. Pegg, Modification of the cellular antioxidant activity (CAA) assay to study phenolic antioxidants in a Caco-2 cell line, *Food Chem.*, 2018, **244**, 359–363, DOI: [10.1016/j.foodchem.2017.10.035](https://doi.org/10.1016/j.foodchem.2017.10.035).
- 20 N. Faubel, M. Makran, R. Barberá, G. Garcia-Llatas, I. C. Giardina, L. Tesoriere, A. Attanzio and A. Cilla, Anti-inflammatory activity of plant sterols in a co-culture model of intestinal inflammation: focus on food-matrix effect, *Food Funct.*, 2024, **15**, 6502–6511, DOI: [10.1039/D4FO00917G](https://doi.org/10.1039/D4FO00917G).
- 21 M. Berkel Kasikci, S. Guilois-Dubois, K. Billet, J. Jardin, S. Guyot and M. Morzel, Interactions between salivary proteins and apple polyphenols and the fate of complexes during gastric digestion, *J. Agric. Food Chem.*, 2024, **72**, 9179–9189, DOI: [10.1021/acs.jafc.4c00468](https://doi.org/10.1021/acs.jafc.4c00468).
- 22 D. de Paulo Farias, F. F. de Araújo, I. A. Neri-Numa, F. L. Dias-Audibert, J. Delafiori, R. R. Catharino and G. M. Pastore, Effect of *in vitro* digestion on the bioaccessibility and bioactivity of phenolic compounds in fractions of eugenia pyriformis fruit, *Food Res. Int.*, 2021, **150**, 110767, DOI: [10.1016/j.foodres.2021.110767](https://doi.org/10.1016/j.foodres.2021.110767).
- 23 T. Tarko and A. Duda-Chodak, Influence of food matrix on the bioaccessibility of fruit polyphenolic compounds, *J. Agric. Food Chem.*, 2020, **68**, 1315–1325, DOI: [10.1021/acs.jafc.9b07680](https://doi.org/10.1021/acs.jafc.9b07680).
- 24 P. Esquivel, M. Viñas, C. B. Steingass, M. Gruschwitz, E. Guevara, R. Carle, R. M. Schweiggert and V. M. Jiménez, Coffee (*Coffea arabica* L.) by-products as a source of carotenoids and phenolic compounds—evaluation of varieties with different peel color, *Front. Sustain. Food Syst.*, 2020, **4**, 590597, DOI: [10.3389/fsufs.2020.590597](https://doi.org/10.3389/fsufs.2020.590597).
- 25 C. I. Victoria-Campos, J. de J. Ornelas-Paz, C. Rios-Velasco, S. Ruiz-Cruz, J. Ornelas-Paz, C. L. Del Toro-Sánchez, E. Márquez-Ríos and R. Calderón-Loera, Relevance of anthocyanin metabolites generated during digestion on bioactivity attributed to intact anthocyanins, *Foods*, 2024, **13**, 4066, DOI: [10.3390/foods13244066](https://doi.org/10.3390/foods13244066).
- 26 C. Gu, H. A. R. Suleria, F. R. Dunshea and K. Howell, Dietary lipids influence bioaccessibility of polyphenols from black carrots and affect microbial diversity under simulated gastrointestinal digestion, *Antioxidants*, 2020, **9**, 762, DOI: [10.3390/antiox9080762](https://doi.org/10.3390/antiox9080762).
- 27 S. Cañas, N. Tosi, V. Núñez-Gómez, D. Del Rio, P. Mena, M. A. Martín-Cabrejas and Y. Aguilera, Microbial catabolism of coffee pulp (poly)phenols during *in vitro* colonic fermentation, *Food Chem.*, 2025, **463**, 141354, DOI: [10.1016/j.foodchem.2024.141354](https://doi.org/10.1016/j.foodchem.2024.141354).



- 28 W. Preedalikit, C. Chittasupho, P. Leelapornpisid, N. Duangnin and K. Kiattisin, Potential of coffee cherry pulp extract against polycyclic aromatic hydrocarbons in air pollution induced inflammation and oxidative stress for topical applications, *Int. J. Mol. Sci.*, 2024, **25**, 9416, DOI: [10.3390/ijms25179416](https://doi.org/10.3390/ijms25179416).
- 29 L. Łyko, M. Olech, U. Gawlik, A. Krajewska, D. Kalembe, K. Tyśkiewicz, N. Piórecki, A. Prokopiv and R. Nowak, Rhododendron luteum sweet flower supercritical CO<sub>2</sub> extracts: terpenes composition, pro-inflammatory enzymes inhibition and antioxidant activity, *Int. J. Mol. Sci.*, 2024, **25**, 9952, DOI: [10.3390/ijms25189952](https://doi.org/10.3390/ijms25189952).
- 30 K. M. Herrera-Rocha, N. E. Rocha-Guzmán, J. A. Gallegos-Infante, R. F. González-Laredo, M. Larrosa-Pérez and M. R. Moreno-Jiménez, Phenolic acids and flavonoids in acetic extract from quince (*Cydonia oblonga* Mill.): nutraceuticals with antioxidant and anti-inflammatory potential, *Molecules*, 2022, **27**, 2462, DOI: [10.3390/molecules27082462](https://doi.org/10.3390/molecules27082462).
- 31 N. Hutachok, P. Angkasith, C. Chumpun, S. Fucharoen, I. J. Mackie, J. B. Porter and S. Srichairatanakool, Anti-platelet aggregation and anti-cyclooxygenase activities for a range of coffee extracts (*Coffea arabica*), *Molecules*, 2020, **26**, 10, DOI: [10.3390/molecules26010010](https://doi.org/10.3390/molecules26010010).
- 32 B. Upadhyaya, R. Moreau and K. Majumder, Antioxidant and anti-inflammatory capacities of three dry bean varieties after cooking and *in vitro* gastrointestinal digestion, *J. Agric. Food Chem.*, 2024, **72**, 18445–18454, DOI: [10.1021/acs.jafc.4c02215](https://doi.org/10.1021/acs.jafc.4c02215).
- 33 S. Zhang, Z. Gai, T. Gui, J. Chen, Q. Chen and Y. Li, Antioxidant effects of protocatechuic acid and protocatechuic aldehyde: old wine in a new bottle, *Evid.-Based Complementary Altern. Med.*, 2021, **2021**, 1–19, DOI: [10.1155/2021/6139308](https://doi.org/10.1155/2021/6139308).
- 34 K. N. Kasapoğlu, J. Kruger, A. Barla-Demirkoz, M. Gültekin-Özgüven, J. Frank and B. Özçelik, Optimization of supercritical carbon dioxide extraction of polyphenols from black rosehip and their bioaccessibility using an *in vitro* digestion/Caco-2 cell model, *Foods*, 2023, **12**, 781, DOI: [10.3390/foods12040781](https://doi.org/10.3390/foods12040781).
- 35 G. Pereira-Caro, S. Cáceres-Jiménez, A. Moreno-Ortega, S. Dobani, K. Pourshahidi, C. I. R. Gill, P. Mena, D. Del Rio, J. M. Moreno-Rojas, G. Taurino, O. Bussolati, T. M. Almutairi, A. Crozier and M. G. Bianchi, Colon-available mango (poly)phenols exhibit mitigating effects on the intestinal barrier function in human intestinal cell monolayers under inflammatory conditions, *Food Funct.*, 2024, **15**, 5118–5131, DOI: [10.1039/D4FO00451E](https://doi.org/10.1039/D4FO00451E).
- 36 S. Mei, D. D. Kitts and X. Chen, Coffee leaf polyphenol-rich extracts alleviated lipopolysaccharide-induced intestinal barrier dysfunction: insights from a Caco-2/U937 co-culture model, *Food Biosci.*, 2024, **61**, 104639, DOI: [10.1016/j.fbio.2024.104639](https://doi.org/10.1016/j.fbio.2024.104639).
- 37 L. Yuan, Q. Chu, B. Yang, W. Zhang, Q. Sun and R. Gao, Purification and identification of anti-inflammatory peptides from sturgeon (*Acipenser schrenckii*) cartilage, *Food Sci. Hum. Wellness*, 2023, **12**, 2175–2183, DOI: [10.1016/j.fshw.2023.03.030](https://doi.org/10.1016/j.fshw.2023.03.030).
- 38 N. Liang and D. Kitts, Role of chlorogenic acids in controlling oxidative and inflammatory stress conditions, *Nutrients*, 2015, **8**, 16, DOI: [10.3390/nu8010016](https://doi.org/10.3390/nu8010016).
- 39 F. Machado, M. A. Coimbra, M. D. del Castillo and F. Coreta-Gomes, Mechanisms of action of coffee bioactive compounds – a key to unveil the coffee paradox, *Crit. Rev. Food Sci. Nutr.*, 2024, **64**, 10164–10186, DOI: [10.1080/10408398.2023.2221734](https://doi.org/10.1080/10408398.2023.2221734).
- 40 I. A. Ludwig, M. N. Clifford, M. E. J. Lean, H. Ashihara and A. Crozier, Coffee: biochemistry and potential impact on health, *Food Funct.*, 2014, **5**, 1695–1717, DOI: [10.1039/C4FO00042K](https://doi.org/10.1039/C4FO00042K).
- 41 J. dePaula and A. Farah, Caffeine consumption through coffee: content in the beverage, metabolism, health benefits and risks, *Beverages*, 2019, **5**, 37, DOI: [10.3390/beverages5020037](https://doi.org/10.3390/beverages5020037).
- 42 G. Zhang, X. Yan, J. Xia, J. Zhao, M. Ma, P. Yu, D. Gong and Z. Zeng, Assessment of the effect of ethanol extracts from *Cinnamomum camphora* seed kernel on intestinal inflammation using simulated gastrointestinal digestion and a Caco-2/RAW264.7 co-culture system, *Food Funct.*, 2021, **12**, 9197–9210, DOI: [10.1039/D1FO01293B](https://doi.org/10.1039/D1FO01293B).
- 43 C. A. Dinarello, Overview of the IL-1 family in innate inflammation and acquired immunity, *Immunol. Rev.*, 2018, **281**, 8–27, DOI: [10.1111/imr.12621](https://doi.org/10.1111/imr.12621).

